

Gastroenterology

Combined activities of JNK1 and JNK2 in hepatocytes protect against toxin-induced liver injury

--Manuscript Draft--

Manuscript Number:	GASTRO-D-14-01639R2
Full Title:	Combined activities of JNK1 and JNK2 in hepatocytes protect against toxin-induced liver injury
Article Type:	Basic - Liver
Section/Category:	Basic
Corresponding Author:	Christian Trautwein, M.D. University Hospital, RWTH Aachen Aachen, GERMANY
Corresponding Author Secondary Information:	
Corresponding Author's Institution:	University Hospital, RWTH Aachen
Corresponding Author's Secondary Institution:	
First Author:	Francisco Javier Cubero
First Author Secondary Information:	
Order of Authors:	Francisco Javier Cubero
	Miguel Eugenio Zoubek
	Jin Peng
	Wei Hu
	Gang Zhao
	Yulia A. Nevzorova
	Malika Al Masaoudi
	Lars P. Bechmann
	Mark V. Boekschoten
	Michael Muller
	Nikolaus Gassler
	Christian Preisinger
	Ali E. Canbay
	Tom Luedde
	Roger J Davis
	Christian Liedtke
	Christian Trautwein, M.D.
Order of Authors Secondary Information:	
Abstract:	Background&Aims: c-Jun N-terminal kinase (JNK)1 and JNK2 are expressed in hepatocytes and have overlapping and distinct functions. JNK proteins are activated, via phosphorylation, in response to acetaminophen- or CCl4-induced liver damage; the level of activation correlates with the degree of injury. SP600125, a JNK inhibitor, has been reported to block acetaminophen-induced liver injury. We investigated the role of JNK in drug-induced liver injury (DILI) in liver tissues from patients and in mice with genetic deletion of JNK in hepatocytes. Methods: We studied liver sections from

patients with DILI (due to acetaminophen, phenprocoumon, non-steroidal anti-inflammatory drugs or autoimmune hepatitis), or patients without acute liver failure (controls), collected from a DILI Biobank in Germany. Levels of total and activated (phosphorylated) JNK were measured by immunohistochemistry and western blotting. Mice with hepatocyte-specific deletion of Jnk1 (Jnk1 Δ hepa) or combination of Jnk1 and Jnk2 (Jnk Δ hepa), as well as Jnk1-floxed C57BL/6 (control) mice, were given injections of CCl₄ (to induce fibrosis) or acetaminophen (to induce toxic liver injury). We performed gene expression microarray, and phosphoproteomic analyses to determine mechanisms of JNK activity in hepatocytes. Results: Liver samples from DILI patients contained more activated JNK, predominantly in nuclei of hepatocytes and in immune cells, than healthy tissue. Administration of acetaminophen to Jnk Δ hepa mice produced a greater level of liver injury than that observed in Jnk1 Δ hepa or control mice, based on levels of serum markers and microscopic and histologic analysis of liver tissues. Administration of CCl₄ also induced stronger hepatic injury in Jnk Δ hepa mice, based on increased inflammation, cell proliferation, and fibrosis progression, compared to Jnk1 Δ hepa or control mice. Hepatocytes from Jnk Δ hepa mice given acetaminophen had an increased oxidative stress response, leading to decreased activation of AMPK, total protein AMPK levels, and pJunD and subsequent necrosis. Administration of SP600125 before or with acetaminophen protected Jnk Δ hepa and control mice from liver injury. Conclusions: In hepatocytes, JNK1 and JNK2 appear to have combined effects in protecting mice from CCl₄- and acetaminophen-induced liver injury. It is important to study the tissue-specific functions of both proteins, rather than just JNK1, in the onset of toxic liver injury. JNK inhibition with SP600125 shows off-target effects.



MEDIZINISCHE KLINIK III

*Schwerpunkt Gastroenterologie, Stoffwechselerkrankungen
Internistische Intensivmedizin*

Direktor: Univ.-Prof. Dr. med. Christian Trautwein

Medizinische Klinik III ♦ Universitätsklinikum ♦ D-52057 Aachen

Aachen, November 16th 2015

Dr. Bishr Omary
Professor and Chair of Molecular & Integrative Physiology
1137 E. Catherine St, Ann Arbor
MI, 48109-5622

Re: GASTRO-D-14-01639-R2

Dear Bishr, Dear Prof. Omary,

Please find attached our revised manuscript GASTRO-D-14-01639-R2 "**Combined activities of JNK1 and JNK2 protect against toxic liver injury**", which we would like you to resubmit to **Gastroenterology**.

In order to address the concerns and suggestions of the Reviewers we have significantly revised the first revised version of the manuscript. Specifically, we have included data to better characterize JNK activation in human DILI and murine APAP-derived liver injury *in vivo* and to understand the mechanism, similar in mice and men. Furthermore, we found that mice with JNK deletion in hepatocytes are more sensitive to APAP-induced liver injury due to a decline in the protein levels of pAMPK and AMPK. However in mice with JNK deletion in hepatocytes pJNK is increased, which is explained by a strong infiltration of JNK-positive immune cells. These results strongly suggest that JNK in non-parenchymal-cells plays an essential role in APAP-induced liver injury. Through the helpful comments of the reviewers and the editors we clarified that SP600125, the classical JNK inhibitor, exerts off-targets effects on AMPK-regulating phosphatases (e.g.: PP2C).

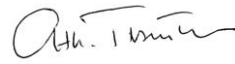
Thus, we think that the helpful Editor's and Reviewer's comments have substantially improved our manuscript. We hope that after addressing all the comments raised after our re-

revised version, our manuscript is now suitable for acceptance in **Gastroenterology**. We are looking forward to your response.

Sincerely yours,



Francisco Javier Cubero



Christian Trautwein

Point-by-point reply to Editors and Reviewers:

Editorial Board:

1. The important human data you show in Fig1A and B need to be compatible and interconnected, and so do the findings in mice and humans. It is important to show JNK activation biochemically in panel B because on one hand, Fig1A suggests activation yet Fig1B shows dramatic decrease in JNK1 and JNK2 protein in the human DILI livers. How could this be? This also relates to point 1 highlighted by Reviewer 2. Its still difficult to tell which cells are positive for pJNK; also please include information as to which p-JNK antibody did you used and the site it recognizes (?pT183/Y185 which presumably recognizes both JNKs.) Therefore, it is essential to: (i) test pJNK in the human livers by immunoblotting. Is it only the inflammatory cells that are activated or is it both hepatocytes and other cells? What percent of the cells are p-JNK positive and have nuclear localization? (ii) In Fig1B: what patients were tested by immune blotting; please specify the DILI type for each lane, (iii) the mouse APAP experiments: it is important to show what happens to JNK1 and JNK2 and their phosphorylation in the APAP model and contrast that with the human findings. One potential issue might be the timing of when specimen are harvested. Definitive conclusions need to be provided. As it stands now, there is some mouse data but its not clear how that matches with human DILI (at least with regard to APAP-related DILI).

Reply: We thank for the comments and apologize for the lack of clarity. In our revised version of the manuscript, we now clearly identified the samples that we used. Liver biopsies from normal liver tissue were labeled as healthy controls (#C1-C4), whereas patients with different etiologies of DILI are also indicated (#1-4). The patients' characteristics are summarized in Suppl. Table 1 and in Figure Legend 1. An experienced pathologists scored the percentage of p-JNK positive cells (hepatocytes vs. non-parenchymal cells; nuclear vs. cytoplasmic). Since most of the pJNK staining was nuclear, the percentage of nuclear staining per view field is shown (n=7-10). Interestingly, we found cytoplasmic JNK staining in ibuprofen-derived DILI liver biopsies.

In summary, in healthy tissue (C1-C4) we found absence or minimal JNK activation. In contrast, DILI-ALF patients (1-4) displayed strong immune cell infiltration associated with pJNK positivity (Figure 1A). Thus, we performed immunoblotting of liver samples of ALF patients with anti-JNK1 and JNK2 antibodies (Figure 1B). DILI-ALF patients displayed increased JNK phosphorylation (pT183/Y185, Cell Signaling Antibody, page 3; Suppl. Material). Interestingly, we detected a differential pattern of JNK1 expression and increased JNK2 levels in livers of DILI-ALF patients (Figure 1B).

We next investigated the similarity of mechanism in human ALF and APAP-derived liver injury in mice. Eight hours after injection of 500 mg/kg APAP, we collected all liver samples (at the same time in liquid nitrogen, which were stored at -80°C). *Wt* mice elicited activation of JNK (same antibody from CTS we used for human samples). Noticeably, mice with specific deletion of *Jnk1* in hepatocytes (*Jnk1*^{Δhepa}) displayed reduced pJNK. In contrast, *Jnk*^{Δhepa} livers showed strong JNK induction, which is explained by strong immune cell infiltration in these mice during APAP-induced liver injury (Figure 1E). Interestingly, we detected increased expression of JNK1 and complete abrogation of JNK2 in *Jnk*^{Δhepa} in murine APAP. Altogether our results indicated that (1) JNK is strongly activated in all forms of DILI-induced ALF, (2) etiology-dependent not only hepatocytes but also immune infiltrating cells are pJNK positive and; (3) Hence, a dysregulation of JNK1 and JNK2 protein expression is characteristic of both human and murine DILI. This is also discussed on Page 18.

2. Your cover letter mentions a 2004 paper by Zhou et al but this reference is not included in the reference list and does not appear to be in PubMed (unless we missed it). What is the overlap between this paper and what is shown in this current manuscript. Related to this, if results related to JNK1-delta are planned for another manuscript, they really should be part of this paper.

Reply: We are sorry for the misunderstanding. The paper we cite is Zhao et al (Gut, 2014). In this paper we showed that JNK1 in hepatocytes has no impact on the progression of CCl₄-induced toxic liver injury, while JNK1 is important for trans-differentiation of hepatic stellate cells (HSCs) and fibrogenesis. Therefore, we believe that there is no overlap between the two manuscripts. However, our findings are very important in light of our previous publication, first demonstrating the specific function of JNK1 in HSCs, and now the combined function of JNK1 and JNK2 in hepatocytes during CCl₄-induced liver injury. We also discussed these findings in different cell types, in the discussion section of the revised version of the manuscript (see page 18).

Its a bit strange to move from JNK1-delta (Fig1 and 2) to JNK2-delta (e.g., Fig3).

In the present study we aimed to address specifically the combined functions of JNK1 and JNK2 in hepatocytes in models of acute and chronic liver toxicity. For the APAP-induced liver injury model, we employed mice with hepatocyte-specific deletion of JNK1 (*Jnk1^{Δhepa}*) and compared them with *Jnk1^{Δhepa}/Jnk2^{-/-}* (*Jnk^{Δhepa}*) and the corresponding wildtype mice. The generation of these mice is specified in page 7 (Material and Methods). *Jnk2^{-/-}* mice were not included in our study since they exhibit a mild protection against APAP (Gunawan, 2006). In addition, mice with hepatocyte-specific deletion of JNK2 are not yet available.

For the chronic toxic liver injury experiments with CCl₄, we compared *Jnk2^{-/-}* with *Jnk1^{Δhepa}/Jnk2^{-/-}* (*Jnk^{Δhepa}*), and the corresponding wildtype mice. Here, *Jnk1^{Δhepa}* were not included since these data have been already published as mentioned before (Zhao, 2014).

3. Page 11 states that CYP2E1 is increased. However, Fig.2E does not really support this. Also, Suppl Fig2B show modest increase at best (similar to one of the immunoblot lanes) but its not clear how many livers were tested. Also, the staining of the CYP is rather diffuse in the JNK-delta which might be coming from damaged hepatocytes. It not clear how relevant is that data given the small changes. What is more important is what happens to JNKs, their phosphorylation and other down-stream targets. Quantification of the histologic liver injury should be included. You can probably remove this data to make room for other more relevant information.

Reply: Thank you. Following the Editorial Board' suggestion we deleted the CYP2E1 data. The necrotic foci were quantified by our pathologist. This information is now included in Fig. 2.

4. The purpose of the experiment shown in Suppl Fig7 is not clear. BM from both WT and JNK-del/hepa should be identical since JNK is presumably deleted only in hepatocytes. The results are not surprising.

Reply: We agree with the Editors that the BMT experiments were expected and thus deleted Suppl. Fig. 7.

5. The validation data (Fig5C) does not really match what is shown in Fig.5B (and some of the mRNA in Suppl Fig.8, such as PCNA, does not match what is shown in Fig.5C). Biologically meaningful conclusions (if indeed there are molecular differences unless basal conditions) need to be clearly shown. This is also compounded by what is shown in Suppl Fig8B,C (panel C does not show the BrdU for the delta-hepa and panel D is shown but not referred to in the text or explained) and stated at the top of page 14 of the manuscript.

Reply: We revisited the Gene Array analysis and the samples we used for the validation. We summarized the findings using the Ingenuity Pathway Analysis™ (IPA) clearly showing that combined deletion of JNK1 and JNK2 in hepatocytes affect the expression of genes associated with cell death and proliferation, as well as inflammation. We found higher expression of

pSTAT3, *Saa2* and *c-myc* (cell cycle), and decreased *BclXL* and *Bad* (apoptosis) in *JNK^{Δhepa}* livers (n=3-5).

We also corrected Suppl. Fig. 9 (former 8) and clearly found reduced BrdU-positive proliferating cells (and thus cell cycle activity) in 48h plated *Jnk^{Δhepa}* hepatocytes (Suppl. Fig. 9C+D).

6. Text refers to Supp Fig9 C+D but the figure shows only panel A. There is also misnumbering related to Suppl Fig10 which made following the text difficult.

Reply: Thank you. This has been now corrected and the former Supp. Fig. 10 deleted.

7. Caspase activation needs to be shown biochemically (as related to the text on page 15). Also, quantification of the TUNEL data should be included (numbers can be included below the panels to minimize the use of space, with p values)

Reply: We have included the TUNEL quantification and caspase-3 activity (fold induction). This is the new Figures 6D-E. We moved the Ann V/EtH III staining and quantification to Suppl. Fig. 10.

8. The protection of *Rip3^{-/-}* hepatocytes from APAP does not mean that SP600125 effect is mediated by RIP3. What happens if you added this compound to *RIP3^{-/-}* hepatocytes? You can probably remove this data to have more space to focus on more relevant information.

Reply: Thank you for your comment, as suggested by the reviewer we deleted the data.

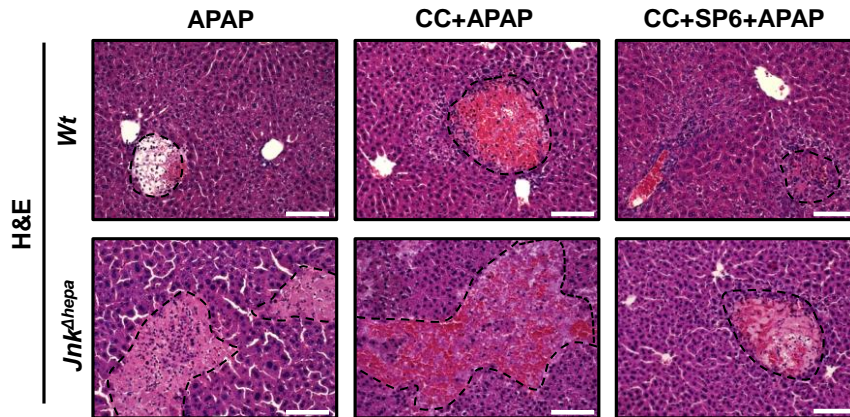
9. One key missing piece remains to be the mechanism. One of your more interesting findings is what appears to be direct or indirect regulation of AMPK by JNK absence even under basal conditions (Fig7D: compare lane 1 with lanes 2 and 3 for pAMPK, assuming this is reproducible; AMPK levels should also be shown). It appears that the SP is acting by inhibition of a phosphatase that is then allowing compensatory phosphorylation of proteins such as AMPK. If AMPK is protective then you should be able to show that experimentally. Hence, the mechanism needs to be explored further with additional data provided. The conclusion should state that SP has off-target effect on AMPK (if that is conclusively shown, which you would need to provide experimentally). Related to this, it would be important to include a schematic as the last panel of Fig7 (Fig7F can be move to the supplemental section) that summarizes your findings.

Reply: Thank you for this important point. Based on your suggestions we included several new experimental approaches. First, we investigated AMPK signaling. Interestingly, AMPK activity was abrogated after APAP challenge in control and *Jnk^{Δhepa}* animals. Total AMPK levels were also affected by APAP treatment. Strikingly, APAP treatment caused a decline in total AMPK levels in *Wt* and dramatically in *Jnk^{Δhepa}* livers. In contrast, co-treatment with SP600125, reversed the APAP-mediated effect on pAMPK and AMPK levels in both *Wt* and *Jnk^{Δhepa}* animals. Next, we examined whether lower AMPK levels correlated with JNK activity. APAP treatment increased JNK in *Wt* and, to a stronger extent, in *Jnk^{Δhepa}* livers, an effect blocked by co-treatment with SP600125.

Collectively, these data suggest that; (1) SP600125 exerts an off-target effect on AMPK, and; (2) The protective effect of SP600125 occurs in liver parenchymal cells. These data are now part of the new Figure 7D+E. We also discuss our results on page 19, indicating that the off-target effect of SP600125 might be a protein phosphatases such as 2C (PP2C) which negative regulate AMPK signaling, preventing the dephosphorylation of AMPK.

Additionally, we confirmed the protective role of AMPK by testing the *in vivo* the effects of pharmacological blockade of AMPK using [20 mg/kg] Compound C (CC), a cell-permeable AMPK inhibitor. As shown in the Fig. for Reviewers only, control and *Jnk^{Δhepa}* animals were

challenged with APAP±SP600125 for 8h. One hour before APAP injection, mice received CC [20 mg/kg] *i.p.*. Inhibition of AMPK by CC resulted in increased areas of necrotic foci in control and to a larger extent in *Jnk^{Δhepa}* liver. This effect was attenuated by SP600125. Altogether these data indicate a protective effect exerted by AMPK in murine APAP-induced liver injury.



***In vivo* treatment with CC exacerbates APAP-induced liver injury in mice with combined JNK1 and JNK2 deletion in hepatocytes.**

Representative H&E staining of liver sections collected from the same mice sacrificed 8h after APAP±SP600125 treatment. Compound C (CC) was administered *i.p.* one hour before. Micrographs were examined by an experienced pathologist. Scale bars 200μm.

10. With regard to point #2 raised by Reviewer 2, it appears that SP acts directly on, and protects, hepatocytes. Therefore, this will likely address the Reviewer concern though effects on non-parenchymal cells are indeed possible.

Reply: We agree with Reviewer 2. Increased JNK phosphorylation in *Jnk^{Δhepa}* mice (see Figures 1 and 7, completely different samples, and replicated at least 3 times) clearly demonstrates that JNK in infiltrating cells is involved in APAP-induced liver injury. This is also discussed in the discussion section (Figure 7E).

11. Minor issues: (a) for the sizing bars in the images (gross, H&E, immunofluorescence), please do not include the size in the image since it will not read well when the figure is reduced (the size should be stated in the legend), (b) Please add the Mr sizes to the blots as per our Instructions to Authors, (c) Fig.1A: the red arrows are difficult to see, (d) Fig.2C (right lower panel): please indicate in the legend that the dotted area represents a necrotic focus, (e) no need to use so many decimals in Fig.5B (e.g., 8.2 instead of 8.172), (f) cJUN should probably be cJUN, JUND should be JunD, (f) brackets in Fig7E don't match the lanes.

Reply: Thank you; we have corrected these points.

Reviewer #1:

The authors attempted to address the two important issues (e.g. Jnk targets and context-dependent action of Jnk in the liver) by performing additional experiments, and the new data partially provide answers. Even though the answers remain largely unknown, the findings in this work indeed show that hepatocyte Jnk1

and 2 act together to protect against some types of liver injury, which is interesting. They also significantly modified the text to avoid overstatements of their data.

Reply: Thank you for your comments. In this revised version we further investigated the mechanism by which *Jnk*^{Δhepa} mice elicit increased liver injury. Interestingly, AMPK activity was abrogated after APAP challenge in control and *Jnk*^{Δhepa} animals. Noticeably, APAP treatment caused a decline in total AMPK levels in *Wt* and dramatically in *Jnk*^{Δhepa} livers. In contrast, co-treatment with SP600125, reversed the APAP-mediated effect on pAMPK and AMPK levels in both *Wt* and *Jnk*^{Δhepa} animals. Next, we examined whether lower AMPK levels correlated with JNK activity. APAP treatment increased JNK in *Wt* and, to a stronger extent, in *Jnk*^{Δhepa} livers. This effect was blocked by co-treatment with SP600125.

Collectively, these data suggest that SP600125 exerts an off-target effect on AMPK. This effect might be mediated via a protein phosphatases such as 2C (PP2C) which negatively regulates AMPK signaling, preventing the dephosphorylation of AMPK. Certainly, these interesting observations need to be further confirmed.

Reviewer #2:

This is a resubmitted manuscript studying the role of JNK1 and JNK2 in drug and toxin-induced liver injury and fibrosis. The authors have addressed the concerns raised from previous reviews. This reviewer still has a couple of comments.

Specific comments:

Figure 1A shows increased JNK expression in DILI patients. However, JNK1 and JNK2 expression seems to decrease in DILI samples by WB analysis. The authors should explain this discrepancy appropriately.

Reply: This is an important point. We further studied pJNK activation in liver samples of patients with different DILI etiologies. Increased pJNK in nuclei of hepatocytes and infiltrating cells was characterized by immunohistochemistry but also by Western blot analyses (new Figure 1). While we observed increased JNK2 expression (new Antibody Cell Signalling, replicated at least 3 times), we detected differential expression of JNK1 in the same samples, indicating a deregulation of JNK1 expression.

Figure 7: JNK1-d-hepa and JNK-d-hepa should express JNK1 in non-parenchymal cells. Therefore, not only JNK-independent effect, the protective effect of SP600125 on these animals might also be due to the effect on non-parenchymal cells, suggesting JNK1 in non-parenchymal cells play an important role in the liver pathology. This has to be discussed.

Reply: We absolutely agree with the Reviewer. Indeed, we investigated murine APAP-induced liver injury in Figures 1 and 7 with respect to JNK activation (pJNK, JNK, JNK1 and JNK2). This revised version of the manuscript clearly shows that the infiltrating cells are involved in APAP-induced liver injury, which is especially evident in *Jnk*^{Δhepa} animals. At present we have no functional data on the role of JNK activation in immune cell. This finding is now also discussed in the discussion section (pages 18-20).

Minor comments:

p. 12, l.18, "CD11" should be "CD11b".

Reply: Thank you, we have renamed it.

Manuscript Number: GASTRO 14-01639R2

Title

**Combined activities of JNK1 and JNK2 in hepatocytes
protect against toxic liver injury**

Short Title: **Redundancy of JNK1 and JNK2 in hepatocytes**

Francisco Javier Cubero¹; Miguel Eugenio Zoubek¹; Jin Peng¹; Wei Hu¹; Gang Zhao¹;
Yulia A. Nevzorova¹; Malika Al Masaoudi¹; Lars P. Bechmann²; Mark V. Boekschoten³;
Michael Muller³; Christian Preisinger⁴; Nikolaus Gassler⁵; Ali E. Canbay²; Tom Luedde¹;
Roger J. Davis⁶; Christian Liedtke¹; Christian Trautwein^{1*}

¹Department of Internal Medicine III, University Hospital, RWTH Aachen, Germany

²Department of Gastroenterology and Hepatology, University Hospital Duisburg-Essen,
Essen, Germany

³Nutrition, Metabolism & Genomics group, Wageningen University, Division of Human
Nutrition, Wageningen, The Netherlands

⁴Proteomics Facility, University Hospital, RWTH Aachen, Germany

⁵Institute of Pathology, University Hospital, RWTH Aachen, Germany

⁶Howard Hughes Medical Institute and University of Massachusetts Medical School,
Worcester, Massachusetts, USA

Grant support: This work was supported by the IZKF (UKA, RWTH Aachen), the SFB/TRR57, the START-Program of the Faculty of Medicine (#691405, RWTH Aachen), the DFG (BE#3967/3-1), the DFG TR 285/10-1 and the DFG-EI/ZUK2/I3TM/SF_15_5_17.

Abbreviations (in alphabetical order): ANOVA: Analysis of variance; AIH: Autoimmune hepatitis; ALF: Acute liver failure; ALT: Alanine aminotransferase; AMPK: adenosine monophosphate-activated protein kinase; AP: Alkaline phosphatase; APAP: Acetaminophen; AST: Aspartate aminotransferase; BMT: Bone marrow transplantation; CCl₄: Carbon tetrachloride; ConA: Concanavalin A; CYP2E1: Cytochrome P450, isoform 2E1; DILI: Drug-induced liver injury; ECM: Extracellular matrix; ES: Embryonic stem cells; GSH: Glutathione; HBV: Hepatitis B virus; HCC: Hepatocellular carcinoma; HCV: Hepatitis C virus; H&E: Hematoxylin and eosin; HRP: Horseradish peroxidase; HSCs: Hepatic stellate cells; JNK: c-Jun N-terminal kinases; *Jnk*^{Δhepa}: Dual deletion of *Jnk1* and *Jnk2* in hepatocytes; *Jnk1*^{Δhepa}: Hepatocyte-specific deletion of *Jnk1*; *Jnk2*^{-/-}: Mice carrying constitutive deletion of *Jnk2*; KC: Kupffer cells; MAPK: Mitogen-activated protein kinases; MMP2: Matrix metalloproteinase-2; NAC: N-acetylcysteine; NAPQI: N-acetyl-p benzoquinone imine; NSAID: non-steroidal anti-inflammatory drug; PCNA: Proliferating cell nuclear antigen; PCR: Polymerase chain reaction; PDGFβ: Platelet derived growth factor-beta; PFA: Paraformaldehyde; PKCα: Protein kinase C-alpha; qPCR: Quantitative real-time PCR analysis; RNS: Reactive nitrogen species; ROS: Reactive oxygen species; αSMA: α-smooth muscle actin; TIMP1: Tissue inhibitor of metalloproteinase-1; TNFα: Tumor necrosis factor-α; TUNEL: TdT-mediated dUTP-biotin nick end labeling.

Correspondence: Francisco Javier Cubero & Christian Trautwein, Department of Internal Medicine III, University Hospital, RWTH Aachen, Pauwelstraße, 30, Aachen 52074,

Germany. Telephone: +49-241-80-80662. Fax: +49-241-80-82455.

E-mail: fcubero@ukaachen.de; ctrautwein@ukaachen.de

Disclosures: The authors declare that they have no competing **personal or financial conflicts of interests.**

Transcript Profiling: Affymetrix microarray data have been deposited with the NCBI Gene Expression Omnibus under accession number GSE59602 (<http://www.ncbi.nlm.nih.gov/geo/query/acc.cgi?acc=GSE59602>).

Authors contributions: F.J.C. generated and acquired data, interpreted the results, analyzed the microarray, and wrote the manuscript. **M.E.Z., W.H. and G.Z.** generated the data. J.P. performed immunostainings and immunoblottings of liver samples with acute liver failure. Y.A.N. acquired and analyzed protein expression. M.A.M performed qPCRs, and RT-PCRs, serum analysis and protein extracts as well as technical assistance in general. L.P.B. and A.E.C. provided the human samples. M.V.B. and M.M. performed the microarray. C.P., M.E.Z. and F.J.C. performed the proteomics analysis and validation. N.G. provided his expertise in pathology. R.J.D. created and provided the Jnk1-floxed mice. **T.L. and C.L.** provided material and critically reviewed the manuscript. C.T. conceived, supervised, co-wrote the manuscript and provided funds for the study.

Abstract:

Background&Aims: c-Jun N-terminal kinase (JNK)1 and JNK2 are expressed in hepatocytes and have overlapping and distinct functions. JNK proteins are activated, via phosphorylation, in response to acetaminophen- or CCl₄-induced liver damage; the level of activation correlates with the degree of injury. SP600125, a JNK inhibitor, has been reported to block acetaminophen-induced liver injury. We investigated the role of JNK in drug-induced liver injury (DILI) in liver tissues from patients and in mice with genetic deletion of JNK in hepatocytes. **Methods:** We studied liver sections from patients with DILI (due to acetaminophen, phenprocoumon, non-steroidal anti-inflammatory drugs or autoimmune hepatitis), or patients without acute liver failure (controls), collected from a DILI Biobank in Germany. Levels of total and activated (phosphorylated) JNK were measured by immunohistochemistry and western blotting. Mice with hepatocyte-specific deletion of *Jnk1* (*Jnk1^{Δhepa}*) or combination of *Jnk1* and *Jnk2* (*Jnk^{Δhepa}*), as well as *Jnk1*-floxed C57BL/6 (control) mice, were given injections of CCl₄ (to induce fibrosis) or acetaminophen (to induce toxic liver injury). We performed gene expression microarray, and phosphoproteomic analyses to determine mechanisms of JNK activity in hepatocytes. **Results:** Liver samples from DILI patients contained more activated JNK, predominantly in nuclei of hepatocytes and in immune cells, than healthy tissue. Administration of acetaminophen to *Jnk^{Δhepa}* mice produced a greater level of liver injury than that observed in *Jnk1^{Δhepa}* or control mice, based on levels of serum markers and microscopic and histologic analysis of liver tissues. Administration of CCl₄ also induced stronger hepatic injury in *Jnk^{Δhepa}* mice, based on increased inflammation, cell proliferation, and fibrosis progression, compared to *Jnk1^{Δhepa}* or control mice. Hepatocytes from *Jnk^{Δhepa}* mice given acetaminophen had an increased oxidative stress response, leading to decreased activation of AMPK, total protein AMPK levels, and pJunD and subsequent necrosis.

Administration of SP600125 before or with acetaminophen protected *Jnk^{Δhepa}* and control mice from liver injury. **Conclusions:** In hepatocytes, JNK1 and JNK2 appear to have combined effects in protecting mice from CCl₄- and acetaminophen-induced liver injury. It is important to study the **tissue-specific** functions of both proteins, rather than just JNK1, **in the onset of toxic liver injury**. JNK inhibition with SP600125 shows off-target effects.

KEYWORDS: APAP, mouse model, gene regulation, pharmacological treatment

Introduction

Acute and chronic liver injury is a growing worldwide problem **despite** the recent advances **for the treatment of** HBV and HCV infection. Especially, the frequency of toxic insults such as alcohol, drugs or obesity is even increasing in the Western World. In the liver, toxic injury triggers death signalling pathways, which may cause apoptosis, necrosis or pyroptosis of hepatocytes^{1, 2}. However, the exact pathomolecular mechanisms determining the mode of cell death are not completely understood.

Liver injury of different aetiology activates JNK - members of the MAPK family. Whereas *Jnk3* is exclusively expressed in the central nervous system, testis and heart, *Jnk1* and *Jnk2* are expressed in hepatocytes eliciting redundant but also distinct functions³⁻⁵. In order to characterise the compound functions of the JNK genes e.g. in hepatocytes, cell type-specific deletion of both *Jnk1* and *Jnk2* is essential. At present, most studies have been performed only using single knockout mice or JNK-specific inhibitors.

Toxic liver injury – acute or chronic – activates the oxidative stress response. Typical examples are acute liver damage after APAP intoxication or chronic liver injury by repetitive CCl₄-injection. APAP-induced injury is related to the formation of highly reactive metabolites through CYP2E1. These toxic **compounds** are normally conjugated and inactivated by glutathione (GSH). In overdose conditions, the conjugation of the reactive metabolites leads to GSH depletion and thus enhances the generation of oxidative (ROS) and nitrosative species (RNS) **triggering** hepatocyte injury⁶. *N*-acetylcysteine (NAC) has been the standard antidote for APAP-induced liver intoxication⁷. NAC exerts its therapeutic effects by restoring depleted hepatic glutathione levels, and thus preventing the accumulation of oxidant species⁷.

Earlier results demonstrated that JNK is strongly activated by APAP correlating with the degree of liver injury⁸. Additionally, *in vivo* experiments evidenced that JNK inhibition blocked APAP-induced liver injury⁹. Thus JNK seems to play an essential role in APAP-induced hepatic damage, supporting the possibility of using JNK inhibitors as a therapeutic approach.

Kluwe *et al*¹⁰ first suggested that JNK is crucial for chronic CCl₄-intoxication, associated with hepatocyte damage, necrosis, inflammation, and end-stage liver fibrosis. JNK activation is not only restricted to hepatocytes. Indeed, we found that *Jnk1* is particularly important for trans-differentiation of hepatic stellate cells (HSCs) since *Jnk1* deletion in HSCs reduces fibrogenesis after chronic CCl₄-intoxication¹¹.

In the present work we aimed to address specifically the yet unexplored dual role of *Jnk1* and *Jnk2* in hepatocytes in models of acute and chronic toxic liver injury in mice, and in patients with DILI. Based on the previous studies, we hypothesized that JNK1 and JNK2 in hepatocytes have redundant functions. For this purpose, we generated *Jnk^{Δhepa}* mice and studied the functional role of the JNK genes in APAP- and CCl₄-induced toxic liver injury *in vivo* and *in culture* using primary hepatocytes.

Material and Methods

Generation of mice, animal experiments and human samples

Alb-Cre and *Jnk2*-deficient mice in a C57BL/6 background were purchased from The Jackson Laboratory (Bar Harbor, ME). Mice with a *floxed* allele of *Jnk1* were constructed by using homologous recombination in ES cells and backcrossed to the C57BL/6J strain as previously described^{12, 13}. These mice were then crossed with *Jnk2*-deficient mice to create *Jnk1^{LoxP/LoxP} /Jnk2^{-/-}* mice. Genomic DNA was examined using PCR amplimers (5'-

CTCAGGAAGAAAGGGCTTATTTTC-3' and 5'-GAACCACTGTTCCAATTTCCATCC-3') to distinguish between the control floxed (*Jnk1⁺*, *Jnk1^f*), and deleted (*Jnk1^Δ*) alleles.

Animal experiments were carried out according to the German legal requirements and animal protection law and approved by the authority for environment conservation and consumer protection of the state of North Rhine-Westfalia (LANUV, Germany). Induction of liver fibrosis was performed in 7-8 week-old age-matched male mice (n=9-10 per group) using CCl₄-injection every 3 days for 4 weeks (0.6 mL/kg, *i.p.*). Control animals were injected with corn oil. The *D*-Galactosamine (GalN)/Lipopolysaccharide (LPS) administration was performed in 7-8 weeks-old male control and *Jnk^{Δhepa}* male animals to induce acute hepatitis. 30 minutes prior to the LPS-injection (20 μg/kg, *i.p.*), GalN (800 μg/kg, *i.p.*) was injected. Mice were sacrificed 8 h after LPS injection. We also performed the APAP-induced liver injury model. After fasting overnight, mice were injected with APAP (500 mg/kg), and sacrificed 8h after treatment. SP600125 was injected 2h (pre-treatment) or at the same time with APAP (co-treatment) at a dose of 30 mg/kg, *i.p.*

Liver paraffin sections were obtained from patients with confirmed diagnosis of DILI (paracetamol, phenprocoumon, non-steroidal inflammatory drugs or autoimmune hepatitis) from the Department of Gastroenterology of the University Hospital Essen, Germany. Patients' clinico-pathologic characteristics were analyzed, summarized and represented in Suppl. Table I.

Statistical analysis

All data are expressed as mean ± standard error of the mean. Statistical significance was determined by two-way analysis of variance (ANOVA) followed by a Student's t test or by one-way ANOVA followed by a Newman-Keuls multicomparison test. *P* values less than 0.05 were considered to be significant.

Results

Expression of JNK in human acute liver failure. Drug-induced liver injury (DILI) is the most common cause of ALF¹⁴. **First**, we studied serum parameters of patients with different ALF etiologies. As indicated in Suppl. Table I, livers from patients suffering **from paracetamol (1), phenprocoumon (2), non-steroidal anti-inflammatory drugs (NSAID) (3), and autoimmune hepatitis (AIH)-induced ALF (4) were investigated**. We observed that the most prominent increase in transaminases was evident in patients with APAP- and AIH-induced ALF, while NSAID- and phenprocoumon-induced ALF patients showed less pronounced changes in serum markers. However, all serum samples showed impaired liver function as evidenced by changes in bilirubin and blood coagulation parameters (**Suppl. Table I**). Noticeably, the patient with APAP intoxication showed dramatically increased GLDH levels and blood coagulation parameters (Suppl. Table I).

We next investigated the JNK activation pattern **in these ALF liver samples (1-4) and normal healthy tissue as control (C1-C4) by performing pJNK staining and quantification** (Figure 1A, **Suppl. Fig. 1A**). Absence or minimal activation of JNK was detectable in healthy tissue. Liver histology of the APAP patient in comparison with the other liver samples showed lower infiltration of immune cells and JNK phosphorylation mainly restricted to hepatocytes (Figure 1A). In contrast, liver samples obtained from other ALF subtypes displayed strong immune cell infiltration associated with pJNK positivity (Figure 1A). In the liver, two JNKs are expressed, **JNK1 and JNK2**. Thus, we performed Western Blot analysis of liver samples of ALF patients with anti-JNK1 and JNK2 antibodies (Figure 1B). **Normal tissue displayed mild JNK phosphorylation, whereas ALF patients displayed higher JNK activation. Interestingly, we detected a differential pattern of JNK1 expression and increased levels of JNK2 in DILI-ALF patients** (Figure 1B).

Deletion of JNK1 and JNK2 in hepatocytes. We next aimed to characterize the functional relevance of JNK activation during toxic liver injury. We generated mice with specific deletion of *Jnk1* in hepatocytes (*Jnk1^{Δhepa}*) and combined *Jnk1* and *Jnk2* knockout mice in hepatocytes (*Jnk^{Δhepa}*) (Figure 1C; Suppl. Fig. 1B+C). To exclude the possibility that *Jnk^{Δhepa}* mice exhibited a phenotype under basal conditions we carefully examined 6-8 weeks female and male *Jnk1^{Δhepa}* and *Jnk^{Δhepa}* mice. Liver histology, serum parameters as well as body weight, and liver versus body weight ratio presented values of normal healthy mice (Suppl. Fig. 2A-F).

Since the human data demonstrated that JNK is strongly activated mainly in hepatocytes during APAP-induced ALF, we sought to translate and compare the human ALF results with APAP-derived liver injury in mice. Eight hours after injecting 500 mg/kg APAP, livers of *Wt* mice elicited JNK activation. Noticeably, mice with specific deletion of *Jnk1* in hepatocytes (*Jnk1^{Δhepa}*) displayed reduced pJNK, whereas *Jnk^{Δhepa}* mice showed strong JNK1 induction, suggesting that the infiltrating compartment is responsible for the activation of the MAPK in experimental murine APAP-derived injury (Figure 1D). Furthermore, we detected JNK1 and JNK2 protein expression after APAP in *Wt*, while the levels of JNK1 were strongly induced in *Jnk^{Δhepa}* mice. Expectedly, JNK2 expression was abrogated in mice lacking JNK in hepatocytes.

Jnk^{Δhepa} mice are sensitized towards acetaminophen-induced liver injury. *Jnk^{Δhepa}* showed significantly exacerbated APAP-induced ALF as evidenced by significantly increased AST, ALT and GLDH levels (Figure 2A). No differences were found in liver versus body weight ratio (Suppl. Fig. 3A). Macroscopically, the surface of *Jnk^{Δhepa}* livers showed severe signs of haemorrhagic bleeding, and microscopically the liver was severely injured with presence of large necrotic foci (Figure 2B-D, respectively).

Acetaminophen is metabolized *via* CYP2E1 to the electrophilic reactive product N-acetyl-p benzoquinone imine (NAPQI)¹⁵. Interestingly, we detected a tendency towards in F2-isoprostanes - a direct marker of oxidative stress¹⁶ - and significantly reduced levels of p38 expression in JNK-depleted hepatocytes after APAP treatment (Figure 2E, Suppl. Fig. 3B+C).

These striking results in APAP-induced DILI prompted us to investigate whether the function of JNK1 and JNK2 is universal or dependent on the context of hepatic injury. Thus, we treated *Jnk^{Δhepa}* mice with D-GalN combined with endotoxin (LPS). Unexpectedly, no differences were observed after D-GalN/LPS treatment in survival, serum markers of liver injury, tissue injury or liver *versus* body weight ratio between both control groups and *Jnk^{Δhepa}* animals. These data suggest that JNK1 and JNK2 in hepatocytes play a prominent protective role especially during toxic liver injury (Suppl. Fig. 4A-E).

*CCl₄-induced chronic liver injury is worsened in mice with combined deletion of Jnk1 and Jnk2 in hepatocytes. Since we previously showed that JNK1 in hepatocytes has no impact on the progression of CCl₄-induced toxic liver injury¹¹, we questioned whether compound function of JNK1 and JNK2 in hepatocytes is implicated in chronic toxic liver injury. 28 days after repetitive CCl₄ treatment, *Jnk^{Δhepa}* livers showed larger numbers and size of necrotic areas compared with *Jnk2^{-/-}* or *Wt* control mice (Figure 3A, Suppl. Fig. 5A). *Jnk^{Δhepa}* livers showed increased collagen deposition as evidenced by Sirius red staining, CollagenIA1 and α-smooth muscle actin (αSMA) protein and mRNA expression (Figure 3B-E, Suppl. Fig. 5B-E). Additional liver fibrosis markers such as hydroxyproline quantification, *Timp1* and *Mmp2* (Figure 3F, Suppl. Fig. 5F) suggested a protective role of*

combined JNK1 and JNK2 activation in hepatocytes during chronic toxic CCl₄-induced liver injury.

Aggravated cell death and compensatory proliferation in $Jnk^{\Delta hepa}$ liver after repetitive CCl₄-injection. To better characterize our findings, we analyzed parameters of cell death and proliferation. TUNEL- and cleaved Caspase3-positive nuclei were significantly enhanced 28 days after CCl₄ treatment in $Jnk^{\Delta hepa}$ livers compared with $Jnk2^{-/-}$ or control mice (Figure 4A-C). Concomitantly, compensatory proliferation examined by Ki-67 staining was significantly increased in $Jnk^{\Delta hepa}$ livers (Figure 4D+E). These results were strengthened by higher mRNA expression of cell cycle markers such as *Pcna* (mRNA) and up-regulation of PCNA and CyclinD protein levels in $Jnk^{\Delta hepa}$ compared with $Jnk2^{-/-}$ or control livers (Figure 4F, Suppl. Fig. 6A+B). Thus loss of JNK1 and JNK2 in hepatocytes resulted in stronger cell death accompanied by an increased proliferative response in the liver.

The inflammatory response is increased in $Jnk^{\Delta hepa}$ livers. Chronic inflammation triggers progression of liver fibrosis¹⁷. After 28 days of CCl₄-injection, we found a significant increase in CD11b- and F4/80-positive cells, putative macrophages/Kupffer cells, in $Jnk^{\Delta hepa}$ compared with $Jnk2^{-/-}$ and control livers (Suppl. Fig. 7A+B). Additionally, $Jnk^{\Delta hepa}$ livers displayed stronger expression of inflammatory markers such as *IL1 α* , *IL1 β* , *Mcp1* and *Tnfa* (Suppl. Fig. 7C-F). Hence, loss of JNK1 and JNK2 in hepatocytes caused severe inflammatory liver injury and fibrosis.

Gene and protein profile of $Jnk^{\Delta hepa}$ livers and hepatocytes in basal conditions. To study the impact of *Jnk* deletion on gene expression in liver and hepatocytes, we performed Affymetrix GeneChip microarray analysis of liver and primary hepatocytes isolated from 8

week-old control and *Jnk*^{Δhepa} mice. This comparison revealed significant changes (-1.5<FC>1.5) in the transcript expression of 355 genes which were up-regulated (197 in liver and 158 in hepatocytes) and 448 down-regulated (171 in liver and 277 hepatocytes) in *Jnk*^{Δhepa} mice (Suppl. Fig. 8A+B). We first performed hierarchical clustering of the JNK substrates commonly up- or down-regulated in both livers and hepatocytes of *Jnk*^{Δhepa} mice. Interestingly, we found significantly reduced transcript levels of JNK target genes including transcription factors *Atf*, *JunD* or *Fos* and apoptotic markers (*Bcl2l13* and *Bid*), and up-regulation of *Gadd45b*, *Saa2* and *Cmyc* (Figure 5A). Moreover, Ingenuity Pathway Analysis™ (IPA) demonstrated that combined deletion of *JNK1* and *JNK2* in hepatocytes affected the expression of genes associated with cell death and proliferation (*Cdkn1a*, *Atf*, *myc*), inflammation (*Smad7*, *IL18*, *Ctgf*, *Cox6b2*) as well as metabolism (*ABCC4*, *CYP2B13*) (Figure 5B).

To validate the main findings of the microarray analysis, protein and mRNA expression was analyzed in both livers and freshly isolated primary hepatocytes from 8 week-old *Wt*, *Jnk1*^{Δhepa} and *Jnk*^{Δhepa} mice revealing enhanced expression of pSTAT3, *Saa2* and *c-myc* (cell cycle), and down-regulation of *BclXL* and *Bad* (apoptosis). As expected, lack of *Mapk9/Jnk2* expression was found in *Jnk*^{Δhepa} mice (Figure 5C, Suppl. Fig. 8C+D).

Morphological changes and mitochondrial damage are aggravated in APAP-treated Jnk^{Δhepa} primary hepatocytes. The acute and chronic toxic models suggested that JNK1 and JNK2 have synergistic functions for hepatocyte protection. We aimed to better define the molecular mechanisms explaining our findings *in vivo*, in primary control (*Wt*) and *Jnk*^{Δhepa} hepatocytes. Liver cells were cultured for up to 48h without treatment (Suppl. Fig. 9A). Lack of *Jnk* expression did not affect viability compared with WT hepatocytes (Suppl.

Fig. 9B). However, basal cell cycle activity was reduced in *Jnk^{Δhepa}* compared to control hepatocytes (Suppl. Fig. 9C+D).

Next, we investigated the mechanism underlying the strong phenotype induced by APAP [10 mM] in *Jnk^{Δhepa}* hepatocytes for up to 48h. 12h after APAP treatment *Jnk^{Δhepa}* hepatocytes evidenced cytoplasmic projections, loss of cell-cell contact and detachment in contrast to polyhedral rounded shaped control hepatocytes (Figure 6A). Up to 24h upon treatment, nuclear condensation or fragmentation was significantly stronger in *Jnk^{Δhepa}* compared to control hepatocytes (not shown).

SP600125, an anthrapyrazolone specific JNK inhibitor, has been shown to protect against APAP-induced ALF in mice¹⁸. Unexpectedly, control and *Jnk^{Δhepa}*-APAP treated hepatocytes were protected to the same extent by co-administration of SP600125+APAP (Figure 6A). APAP mediates its toxic effect by forming highly reactive metabolites. Concomitant with the morphological changes, we detected a significant increase in mitochondrial ROS in APAP-treated *Jnk^{Δhepa}* compared with control hepatocytes. Additionally, SP600125 significantly reduced the changes in mitochondrial membrane potential in both control and *Jnk^{Δhepa}* APAP-treated hepatocytes (Figure 6B, Suppl. Fig. 10A).

APAP exacerbates necrotic cell death in Jnk^{Δhepa}-primary hepatocytes. TUNEL staining evidenced significant lower cell survival of APAP-treated *Jnk^{Δhepa}* compared with control hepatocytes 12h after treatment (Figure 6C). Cell death was significantly reduced after SP600125±APAP co-administration in control and *Jnk^{Δhepa}* hepatocytes (Figure 6C+D). We next sought to define the mode of cell death in APAP-treated hepatocytes. We first tested Caspase3 activity before and after APAP administration including SP600125. APAP-treatment in any combination and at different time points did not significantly change

Caspase3 activity (Figure 6E). This result was further confirmed by Caspase3 immunostaining (not shown). To detect the relevance of necrotic cell death, we performed Annexin V/Ethidium Homodimer III staining. The amount of double positive (i.e. necrotic) hepatocytes were significantly higher in *Jnk^{Δhepa}* compared with control hepatocytes, while SP600125 blocked necrosis in both control and *Jnk^{Δhepa}* hepatocytes (Suppl. Fig. 10B+C).

Receptor interacting protein 3 (RIP3) plays an essential role in mediating necrotic cell death. We studied RIP3 and RIP1 expression in WT and *Jnk^{Δhepa}* hepatocytes before and after APAP±SP600125 co-treatment (Figure 6F). APAP treatment had no effect on RIP3, but stimulated RIP1 expression in both control and was strongly induced in *Jnk^{Δhepa}* hepatocytes. SP600125+APAP co-treatment strongly reduced RIP3 expression to comparable levels in control and *Jnk^{Δhepa}* hepatocytes, while the decreasing effect on the RIP1 protein was more prominent in control hepatocytes (Figure 6F).

To characterize the specificity of our findings, we included pERK and p65 expression in our analysis. APAP treatment stimulated both pERK and p65 expression independent of SP600125 co-treatment, suggesting that both pathways are of minor relevance in explaining the effect on necrosis (Figure 6F). To further confirm this result we tested pJNK and p-cJUN expression before and after treatment. As shown in Figure 6F, APAP- induced pJNK and p-cJUN activation in control hepatocytes, while SP600125 blocked JNK, but not cJUN phosphorylation. In contrast, no significant pJNK and p-cJUN expression in either treatment conditions was evident in *Jnk^{Δhepa}* hepatocytes.

In vivo treatment with SP600125 suppresses APAP-induced liver injury in mice with compound deletion of JNK1 and JNK2 in hepatocytes. To validate the *in vitro* findings, we studied SP600125 co- and pre-administration with APAP in *Jnk^{Δhepa}* animals *in vivo*. Co-treatment with the JNK inhibitor provided protection in control and *Jnk1^{Δhepa}* but also in

Jnk^{Δhepa} mice against APAP-induced liver injury (Figure 7A-C). To exclude the possibility that SP600125 affects APAP metabolism, we pre-administered SP600125 to control, *Jnk1^{Δhepa}* and *Jnk^{Δhepa}* mice, and two hours later we injected APAP (Figure 7A-C). However, pre-administration did not affect the protective effect. Noticeably, the number of necrotic foci was largely reduced in liver parenchyma of SP600125 co- or pre-treated *Jnk^{Δhepa}* mice (Figure 7B+C).

Since our results suggested that SP600125 protects against APAP-induced liver injury via JNK-independent mechanisms, we explored other pathways associated with APAP-toxicity. Sabery and colleagues¹⁹ recently showed that the interplay between PKC α and JNK mediates APAP-induced liver injury. PKC α activation increased after APAP treatment and was attenuated by SP600125 co-administration in *Wt* livers (Figure 7D). Moreover, AMPK activity – protective against APAP hepatotoxicity – was abrogated after APAP challenge in control and *Jnk^{Δhepa}* animals. Total AMPK levels were also affected by APAP treatment. Noticeably, APAP treatment caused a decline in total AMPK levels in *Wt* and dramatically in *Jnk^{Δhepa}* livers. In contrast, co-treatment with the classical JNK inhibitor, SP600125, reversed the APAP-mediated effect on pAMPK and AMPK levels in both *Wt* and *Jnk^{Δhepa}* animals.

Next, we examined whether lower AMPK levels correlated with JNK activity. APAP treatment increased JNK in *Wt* and, to a higher extent, in *Jnk^{Δhepa}* livers, an effect blocked by co-treatment with SP600125 (Figure 7D). Collectively, these data suggest that; (1) SP600125 exerts an off-target effect on AMPK, and; (2) the protective effect of SP600125 occurs in liver parenchymal cells.

Lack of JunD activation in APAP-treated Jnk^{Δhepa} murine hepatocytes. We performed a set of quantitative phosphoproteomics experiments to characterize proteins which could be

differentially phosphorylated after APAP treatment in control and *Jnk^{Δhepa}* hepatocytes (Suppl. Fig. 11A). Amongst several differentially phosphorylated proteins, which we could not validate by western blot due to lack of commercially available phospho-antibodies, our screening approach identified JunD – a known JNK nuclear substrate – to be substantially less phosphorylated in APAP-treated *Jnk^{Δhepa}* hepatocytes (Figure 7E). In addition, we investigated overall phosphorylation of MAPKs, which are known substrates of JNK, using a MAPK-substrate specific antibody (Suppl. Fig. 11B). This approach revealed at least nine proteins with reduced phosphorylation in APAP-treated *Jnk^{Δhepa}* hepatocytes. The identity of these proteins was estimated by comparison of their appropriate molecular weights with known JNK substrates (Suppl. Fig. 11B). In summary, these results demonstrate substantially attenuated phosphorylation of JunD and other proteins in APAP-treated *Jnk^{Δhepa}* hepatocytes, which need to be identified in future studies. These findings indicate that a JNK-JunD dependent mechanism might be involved in protecting against APAP-induced liver injury.

Discussion

Acetaminophen- and CCl₄-induced liver injury have been extensively studied since APAP overdose is the leading cause of DILI in the United States and accidental CCl₄ ingestion still occurs¹⁴. An overwhelming amount of evidence demonstrated that JNK activation plays a major role in toxic liver injury²⁰. Our first investigations using human DILI liver samples showed activation of JNK (pJNK) predominantly in nuclei of hepatocytes and in infiltrating cells. These results are in line with observations that JNK activation is not only limited to hepatocytes but also found in pro-fibrotic and inflammatory cells during progression of liver disease in humans and mice^{10, 11, 21}.

Noticeably, our results suggest differential pattern of JNK1 expression, and increased JNK2 levels in human DILI-ALF liver biopsies compared with normal tissue. Furthermore, JNK activation was a common feature of murine APAP-induced liver injury not only in *Wt* but also especially in *Jnk^{Δhepa}* mice. Noticeably, the intense JNK phosphorylation as well as increased JNK1 expression in *Jnk^{Δhepa}* livers after APAP correlated with the dramatic increase in transaminases. These results suggest that JNK1 phosphorylation in infiltrating cells and non-parenchymal cells correlates with the degree of liver injury. However, the functional role of these cell compartments during APAP-induced liver injury needs to be further addressed.

As found in human samples, JNK1 and JNK2 protein expression was also dysregulated after APAP challenge in mice, indicating an analogous mechanism between human and murine DILI. Altogether our results indicated that (1) JNK is strongly activated in all forms of human DILI-induced ALF, (2) etiology-dependent not only hepatocytes but also immune infiltrating cells are pJNK positive and (3) hence, a dysregulation of JNK1 and JNK2 protein expression is characteristic of both human and murine DILI.

Additionally, our array analysis led us to the working hypothesis that JNK1 and JNK2 might have distinct and shared essential functions in hepatocytes. In the **current** study, we found that combined JNK1 and JNK2 deletion in hepatocytes triggers more severe liver injury, inflammation and progression **after repetitive CCl₄ injection**. **Interestingly**, our previous publication revealed that JNK1 is involved in HSCs **trans-differentiation** into collagen-producing myofibroblasts¹¹, associated with reduced liver injury. **Consequently**, JNK2 expression is sufficient to rescue the loss of **JNK1 in hepatocytes** and protects from CCl₄-mediated cell death.

The prominent role of necrotic cell death in APAP-dependent liver injury has been shown in several studies²²⁻²⁶. Previous reports by the lab of Kaplowitz²⁷ suggested that

disruption of JNK2, but not of JNK1, partially prevented APAP-induced liver injury, indicating that targeting JNK2 could be a promising therapeutic approach. **In contrast**, Henderson and collaborators found **no differences in** APAP-induced liver injury **between** *Jnk1*^{-/-} and *Jnk2*^{-/-} mice²⁸. Our data demonstrate that lack of JNK1 and JNK2 expression in hepatocytes caused extensive necrosis within 8h after APAP injection. **Concomitant with these findings, we observed a dramatic oxidative stress response in the liver of *Jnk*^{Δhepa} mice, associated with necrotic cell death^{22, 23}. We excluded that apoptotic cell death plays a significant role in APAP-treated *Jnk*^{Δhepa} hepatocytes.** Instead, we demonstrate that combined JNK1 and JNK2 **activities are** protective against APAP-induced necrotic cell death of hepatocytes by controlling the oxidative stress response.

The observations found in APAP-induced liver injury were specific for this form of ALF, since we observed no differences in the acute hepatitis-D-GalN/LPS model between *Jnk*^{Δhepa} and control animals. This is in agreement with a recent study indicating that combined deletion of JNK1 and JNK2 in hepatocytes did not alter ConA- or LPS-induced liver injury²⁹. However, hematopoietic deficiency in JNK1 and JNK2 prevented ConA-induced liver injury by suppressing TNF production²⁹. These findings clearly suggest that, under certain conditions (e.g. aetiology of liver disease), JNK activation in **infiltrating cells** rather than in hepatocytes is critical. Altogether these results suggest that the context-specific activation of JNK in different cell-types during ALF is essential, and needs to be further defined.

To better assess these results, we included the **classical** JNK inhibitor, SP600125, in our analysis. This compound has been reported to target the highly conserved ATP-binding sites of JNK and protects from APAP-induced liver injury *in vivo*³⁰. Surprisingly, SP600125 was found to confer protection not only to control but also to *Jnk*-deleted hepatocytes *in vivo* and *in vitro*. Moreover, pre-administration of SP600125 did not affect

APAP metabolism. These results suggested that the beneficial effect of SP600125 on APAP-induced liver injury likely results through off-target effects, e.g., on AMPK. Concomitant with previous reports¹⁹, we found decreased levels of pAMPK and a further decline of total AMPK levels – protective against APAP hepatotoxicity– in *Jnk^{Δhepa}* livers, indicating that survival pathways are reduced in animals with JNK deficiency in hepatocytes. Thus SP600125 might act on protein phosphatases such as 2C (PP2C) which negative regulate AMPK signalling, preventing the dephosphorylation of AMPK (Figure 7F).

Additionally, we employed functional proteomics to map differential phosphorylation caused by APAP treatment in JNK-deficient hepatocytes. Our findings suggest repression of JunD activation, another protective element and part of the cell stress response, was further decreased in the absence of JNK in hepatocytes. Hence, the role of other kinases involved in necrotic cell death such as RIP3, RIP1 or MLKL are currently under intensive investigation^{24, 31}.

In summary, we demonstrate that combined JNK1 and JNK2 activation is essential to protect hepatocytes from acute and chronic toxic liver injury *in vivo* and *in vitro*. Our results show that JNK inhibition is a questionable treatment option for APAP-induced liver injury as the protecting effect of SP600125, the classical JNK inhibitor, is mediated by off-target effects. Hence our results show that the cell-type specific function of JNK is a potential therapeutic target. However, the context-specific function needs to be defined before these options can be employed in the clinic.

Acknowledgements

We would like to thank Prof. Neil Kaplowitz for helpful discussion, and Dr. Svenja Sydor, Dr. Henning W. Zimmermann and Johanna Reissing for the samples from patients with

ALF-DILI. The Proteomics Core Facility is supported by a grant from the Interdisciplinary Centre for Clinical Research within the faculty of Medicine at the RWTH Aachen University. F.J.C. is a Ramón y Cajal Researcher (RYC-2014-15242).

References

1. Fink SL, Cookson BT. Apoptosis, pyroptosis, and necrosis: mechanistic description of dead and dying eukaryotic cells. *Infect Immun* 2005;73:1907-16.
2. Guicciardi ME, Malhi H, Mott JL, et al. Apoptosis and necrosis in the liver. *Compr Physiol* 2013;3:977-1010.
3. Conze D, Krahl T, Kennedy N, et al. c-Jun NH(2)-terminal kinase (JNK)1 and JNK2 have distinct roles in CD8(+) T cell activation. *J Exp Med* 2002;195:811-23.
4. Davis RJ. Signal transduction by the JNK group of MAP kinases. *Cell* 2000;103:239-52.
5. Jaeschke A, Rincon M, Doran B, et al. Disruption of the Jnk2 (Mapk9) gene reduces destructive insulinitis and diabetes in a mouse model of type I diabetes. *Proc Natl Acad Sci U S A* 2005;102:6931-5.
6. Reid AB, Kurten RC, McCullough SS, et al. Mechanisms of acetaminophen-induced hepatotoxicity: role of oxidative stress and mitochondrial permeability transition in freshly isolated mouse hepatocytes. *J Pharmacol Exp Ther* 2005;312:509-16.
7. Heard KJ. Acetylcysteine for acetaminophen poisoning. *N Engl J Med* 2008;359:285-92.
8. Matsumaru K, Ji C, Kaplowitz N. Mechanisms for sensitization to TNF-induced apoptosis by acute glutathione depletion in murine hepatocytes. *Hepatology* 2003;37:1425-34.
9. Hanawa N, Shinohara M, Saberi B, et al. Role of JNK translocation to mitochondria leading to inhibition of mitochondria bioenergetics in acetaminophen-induced liver injury. *J Biol Chem* 2008;283:13565-77.
10. Kluwe J, Pradere JP, Gwak GY, et al. Modulation of hepatic fibrosis by c-Jun-N-terminal kinase inhibition. *Gastroenterology* 2010;138:347-59.
11. **Zhao G, Hatting M**, Nevzorova YA, et al. Jnk1 in murine hepatic stellate cells is a crucial mediator of liver fibrogenesis. *Gut* 2014;63:1159-72.
12. Das M, Jiang F, Sluss HK, et al. Suppression of p53-dependent senescence by the JNK signal transduction pathway. *Proc Natl Acad Sci U S A* 2007;104:15759-64.
13. Das M, Sabio G, Jiang F, et al. Induction of hepatitis by JNK-mediated expression of TNF-alpha. *Cell* 2009;136:249-60.
14. Larson AM, Polson J, Fontana RJ, et al. Acetaminophen-induced acute liver failure: results of a United States multicenter, prospective study. *Hepatology* 2005;42:1364-72.
15. Lee SS, Buters JT, Pineau T, et al. Role of CYP2E1 in the hepatotoxicity of acetaminophen. *J Biol Chem* 1996;271:12063-7.
16. Bansal S, Liu CP, Sepuri NB, et al. Mitochondria-targeted cytochrome P450 2E1 induces oxidative damage and augments alcohol-mediated oxidative stress. *J Biol Chem* 2010;285:24609-19.

17. Sunami Y, Leithauser F, Gul S, et al. Hepatic activation of IKK/NF-kappaB signaling induces liver fibrosis via macrophage-mediated chronic inflammation. *Hepatology* 2012.
18. **Xu JJ, Hendriks BS**, Zhao J, et al. Multiple effects of acetaminophen and p38 inhibitors: towards pathway toxicology. *FEBS Lett* 2008;582:1276-82.
19. **Saberi B, Ybanez MD**, Johnson HS, et al. Protein kinase C (PKC) participates in acetaminophen hepatotoxicity through c-jun-N-terminal kinase (JNK)-dependent and -independent signaling pathways. *Hepatology* 2014;59:1543-54.
20. Seki E, Brenner DA, Karin M. A liver full of JNK: signaling in regulation of cell function and disease pathogenesis, and clinical approaches. *Gastroenterology* 2012;143:307-20.
21. Toivola DM, Ku NO, Resurreccion EZ, et al. Keratin 8 and 18 hyperphosphorylation is a marker of progression of human liver disease. *Hepatology* 2004;40:459-66.
22. Kon K, Kim JS, Jaeschke H, et al. Mitochondrial permeability transition in acetaminophen-induced necrosis and apoptosis of cultured mouse hepatocytes. *Hepatology* 2004;40:1170-9.
23. Ni HM, Bockus A, Boggess N, et al. Activation of autophagy protects against acetaminophen-induced hepatotoxicity. *Hepatology* 2012;55:222-32.
24. Ramachandran A, McGill MR, Xie Y, et al. Receptor interacting protein kinase 3 is a critical early mediator of acetaminophen-induced hepatocyte necrosis in mice. *Hepatology* 2013;58:2099-108.
25. **Antoine DJ, Jenkins RE, Dear JW**, et al. Molecular forms of HMGB1 and keratin-18 as mechanistic biomarkers for mode of cell death and prognosis during clinical acetaminophen hepatotoxicity. *J Hepatol* 2012;56:1070-9.
26. McGill MR, Sharpe MR, Williams CD, et al. The mechanism underlying acetaminophen-induced hepatotoxicity in humans and mice involves mitochondrial damage and nuclear DNA fragmentation. *J Clin Invest* 2012;122:1574-83.
27. Gunawan BK, Liu ZX, Han D, et al. c-Jun N-terminal kinase plays a major role in murine acetaminophen hepatotoxicity. *Gastroenterology* 2006;131:165-78.
28. Henderson NC, Pollock KJ, Frew J, et al. Critical role of c-jun (NH2) terminal kinase in paracetamol- induced acute liver failure. *Gut* 2007;56:982-90.
29. Das M, Garlick DS, Greiner DL, et al. The role of JNK in the development of hepatocellular carcinoma. *Genes Dev* 2011;25:634-45.
30. Ishii M, Suzuki Y, Takeshita K, et al. Inhibition of c-Jun NH2-terminal kinase activity improves ischemia/reperfusion injury in rat lungs. *J Immunol* 2004;172:2569-77.
31. Dara L, Johnson H, Suda J, et al. Receptor interacting protein kinase 1 mediates murine acetaminophen toxicity independent of the necrosome and not through necroptosis. *Hepatology* 2015:doi: 10.1002/hep.27939.

Author names in bold designate shared co-first authors

Figure Legends

Figure 1. Expression of JNK during human and murine drug-induced liver injury (DILI). (A) Activation of pJNK in liver samples of ALF patients with different aetiologies: normal liver tissue (C1, C2), paracetamol (1), phenprocoumon (2), autoimmune hepatitis (AIH) (3), and non-steroidal anti-inflammatory drug (NSAID) (4). Scale bars: 50µm. Phospho-JNK positive nuclei were quantified as the average number of hepatocytes or infiltrating cells with dark brown DAB signal per view field of liver sections from healthy and DILI patients. (B) Immunoblotting for pJNK, JNK1 and JNK2 was performed in normal liver tissue (C1-C4) and in liver samples of DILI patients (1-4). (C) Protein expression of JNK1 and JNK2 was assessed in primary hepatocytes (left panel) and livers (right panel) from 8 week-old control (*Wt*), *Jnk2*^{-/-}, *Jnk1*^{Δhepa} and *Jnk*^{Δhepa} mice. Total JNK1 and JNK2 protein levels were determined in whole liver extracts. GAPDH was used as loading control. (D) Immunoblotting for pJNK, JNK1 and JNK2 was performed in liver samples from control (*Wt*), *Jnk1*^{Δhepa} and *Jnk*^{Δhepa} mice treated with APAP for 8h (n=6). GAPDH was used as loading control.

Figure 2. *Jnk*^{Δhepa} mice are sensitized towards acetaminophen-induced liver injury. (A) Serum ALT (left), AST (center) and GLDH (right) levels were determined 8h after APAP challenge in control (*Wt*), *Jnk1*^{Δhepa} and *Jnk*^{Δhepa} livers (n=10). (B) Representative macroscopic view of a liver from each group. Scale bars: 10mm. (C) Representative H&E staining of liver sections collected from mice sacrificed 8h after APAP challenge and examined by an experienced pathologist. Scale bars: 50µm (upper panel) and 100µm (lower panel), respectively. Dotted area represents a necrotic focus. (D) The area of necrosis was quantified in the same mice. (E) Protein levels of pP38 were determined by

Western Blot in APAP-treated control (*Wt*) and *Jnk^{Δhepa}* livers. GAPDH was used as loading control. Data are expressed as mean±SEM (*p<0.05 and **p<0.01).

Figure 3. Liver fibrogenesis is aggravated in *Jnk^{Δhepa}* after chronic CCl₄ treatment.

(A) Representative H&E staining of liver sections of control (*Wt*), *Jnk2^{-/-}* and *Jnk^{Δhepa}* livers, 28 days after repeated injections of CCl₄. Corn-oil injections were used as controls. **Scale bars: 100μm.** **(B)** Representative Sirius red staining of paraffin sections from the same livers. **Scale bars: 100μm.** **(C)** A representative Collagen IA1 staining of frozen sections from the same mice is shown. **Scale bars: 200μm.** **(D)** In addition, mRNA levels for *Collagen IA1* and *αSMA* were determined by qRT-PCR. **(E)** Protein levels of *αSMA* were determined. GAPDH was used as a loading control. **(F)** Hydroxyproline contents were assessed in the same livers. Data are expressed as mean±SEM (*p<0.05 and ***p<0.001).

Figure 4. Cell death and compensatory proliferation are exacerbated after combined deletion of JNK1 and JNK2 in hepatocytes.

(A) Representative TUNEL staining performed on frozen liver sections (upper; **Scale bars: 100μm**) and cleaved CASPASE3 immunohistochemistry in paraffin sections (lower panel; **Scale bars: 100μm**) of control (*Wt*), *Jnk2^{-/-}* and *Jnk^{Δhepa}* livers after 4 weeks of repeated CCl₄ injections are shown. **Quantification of TUNEL- (left) (B) and Caspase3 enzyme activity (C) was analyzed in 4-week CCl₄ treated control (Wt), *Jnk2^{-/-}* and *Jnk^{Δhepa}* livers.** **(D)** Representative Ki-67 staining performed on frozen liver sections of the same livers. **Scale bars: 100μm.** **(E)** Quantification of Ki-67 positive cells per view field is shown. **(F)** Protein levels of PCNA and *CyclinD* were determined by Western Blot in the same samples. GAPDH was used as a loading control. Data are expressed as mean±SEM (***p<0.001). **Arrows denote positive cells.**

Figure 5. Microarray analysis of *Jnk*^{Δhepa} livers and hepatocytes manifest dysregulation in cell proliferation, apoptosis and inflammation at basal levels. (A)

Gene array analysis was performed in 8 week-old control (*Wt*) and *Jnk*^{Δhepa} liver and primary isolated hepatocytes. Correlation of the fold induction of genes in hepatocytes and liver is shown. Log₂ expression values of the individual mice were divided by the mean of the sham-operated mice. Log ratios were saved in a txt file and analyzed with the Multiple Experiment Viewer. Top up- and down-regulated JNK-target substrates are shown (Red: Up-regulated; Blue: Down-regulated, n=3, -1.5<FC>1.5). **(B)** Ingenuity Pathway Analysis™ (IPA) was performed in the same samples and the expression values (in brackets) of the top up- and down-regulated genes in liver (left panel) and primary isolated hepatocytes (right panel) are represented. **(C)** Liver and hepatocytic protein extracts of untreated control (*Wt*), *Jnk1*^{Δhepa} and *Jnk*^{Δhepa} were prepared. The protein expression levels of pStat3, c-myc and Bcl-XL were determined by Western Blot. GAPDH was used as loading control. **(D)** mRNA expression was determined in liver tissue and primary hepatocytes of untreated 8 week-old control (*Wt*), *Jnk1*^{Δhepa} and *Jnk*^{Δhepa} mice. The mRNA expression levels of *Saa2*, *Cmyc* and *BclXL* are shown (n=3-5; *p<0.05; **p<0.01; ***p<0.001).

Figure 6. APAP modifies the morphology and exacerbates mitochondrial damage and necrotic cell death in primary *Jnk*^{Δhepa} hepatocytes. (A)

Primary hepatocytes were isolated from control (*Wt*) and *Jnk*^{Δhepa} mice. A total number of 500.000 cells were seeded in 6-well plates and cultivated for up to 12h. Visible light microphotographs were taken in presence or absence of APAP and/or SP600125. **Scale bars: 200μm.** **(B)** At the same time we performed MitoSox® staining to assess mitochondrial damage (red –arrows–, counter-stained with DAPI, blue). Microphotographs were taken **(scale bars: 100μm).** **(C)** TUNEL

staining was performed. Scale bars: 200 μ m. (D) TUNEL-positive cells were evaluated in the same mice and represented in percentage per view field. (E) The enzyme activity of Caspase3 was measured in frozen tissue. (F) Hepatocytic protein extracts were collected and treated with APAP for 8h in culture in presence or absence of APAP and/or SP600125. The protein expression levels of RIP3, RIP1, p65, pJNK, p-cJUN and pERK were determined by Western Blot. β -actin was used as a loading control.

Figure 7. *In vivo* treatment with SP600125 suppresses APAP-induced liver injury in mice with combined JNK1 and JNK2 deletion in hepatocytes. (A) Serum AST (left) and ALT (right) levels were determined in control (*Wt*), *Jnk1 Δ hepa* and *Jnk Δ hepa* mice injected with SP600125 at the same time as APAP or pre-treated with SP600125, 2h before APAP challenge. Comparison with DMSO and APAP-treated mice is shown (n=10). (B+C) Representative H&E staining of liver sections collected from the same mice sacrificed 8h after treatment and examined by an experienced pathologist. Scale bars: 50 (upper panels) and 200 μ m (lower panels), respectively. Dotted areas represent necrotic foci. (D) Liver extracts were collected and immunoblotting was performed, and the protein levels of PKC α , pAMPK, AMPK and pJNK determined by Western Blot. (E) Phosphorylation of JunD was performed in hepatocytic extracts. GAPDH was used as loading control. (F) APAP triggers higher PKC α , and lower AMPK – a survival pathway- expression inducing JNK phosphorylation and cell death. The JNK classical inhibitor SP600125 exerts an off-target effect by facilitating phosphorylation of AMPK and preventing JNK phosphorylation in hepatocytes.

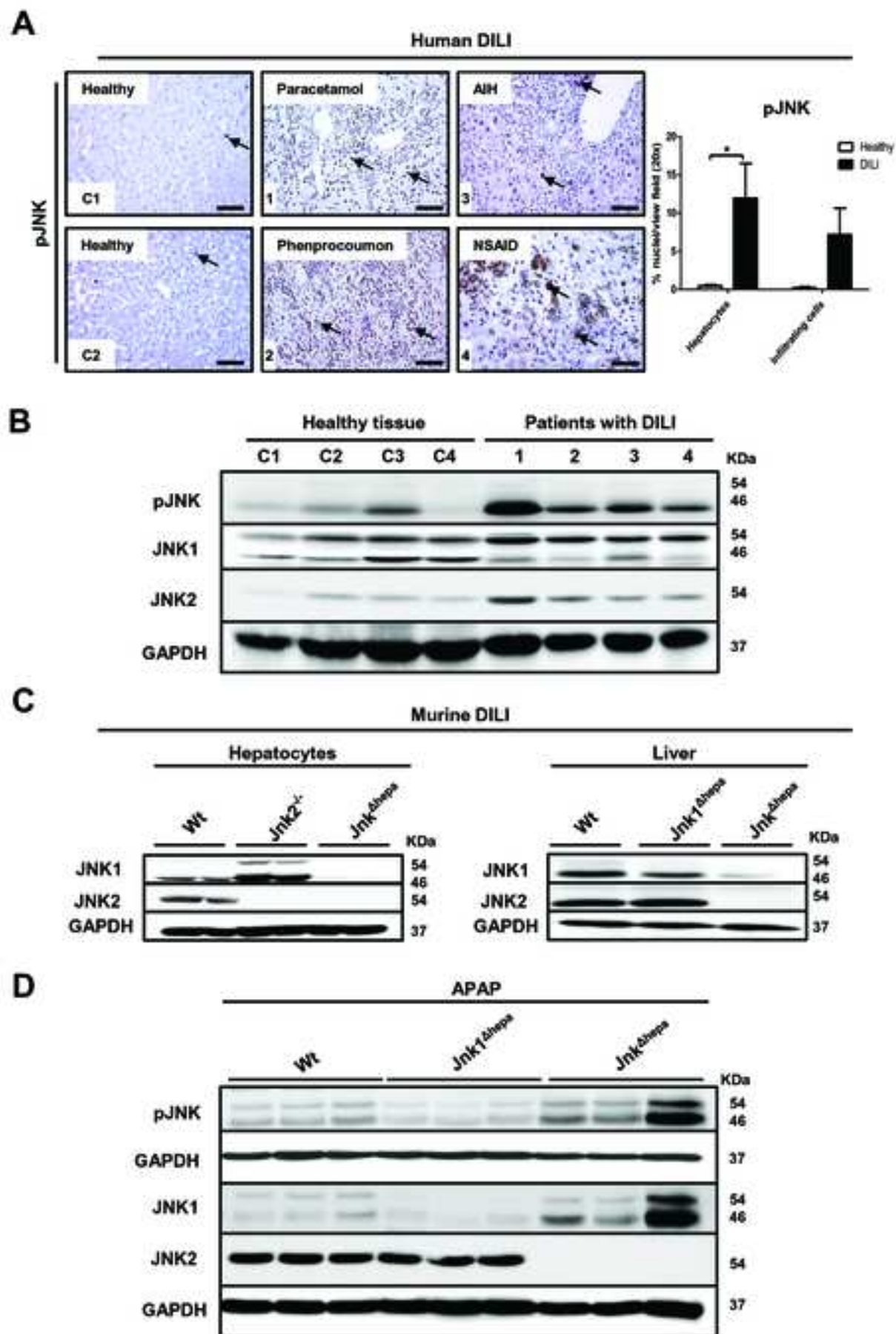


Figure 1

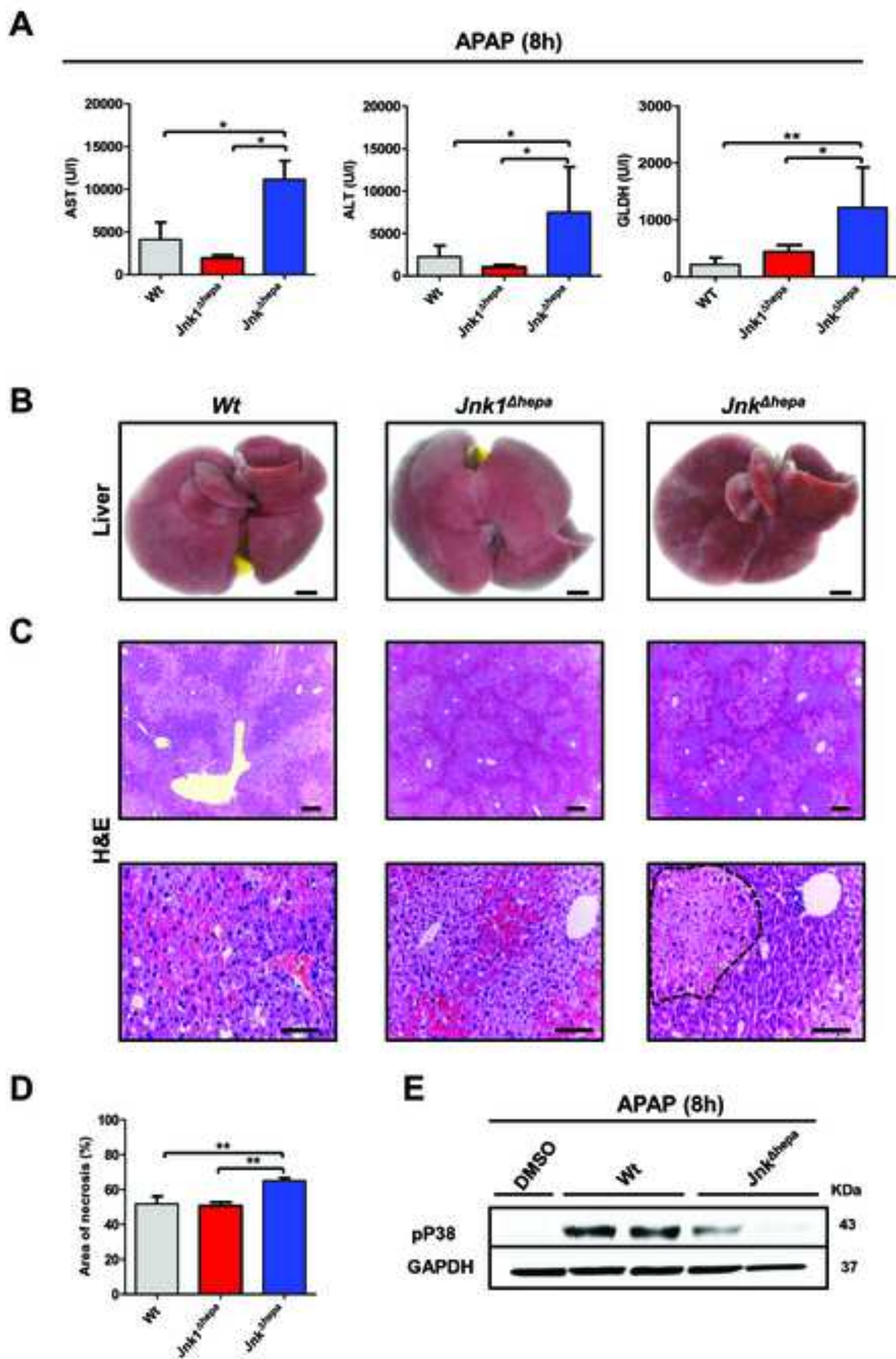


Figure 2

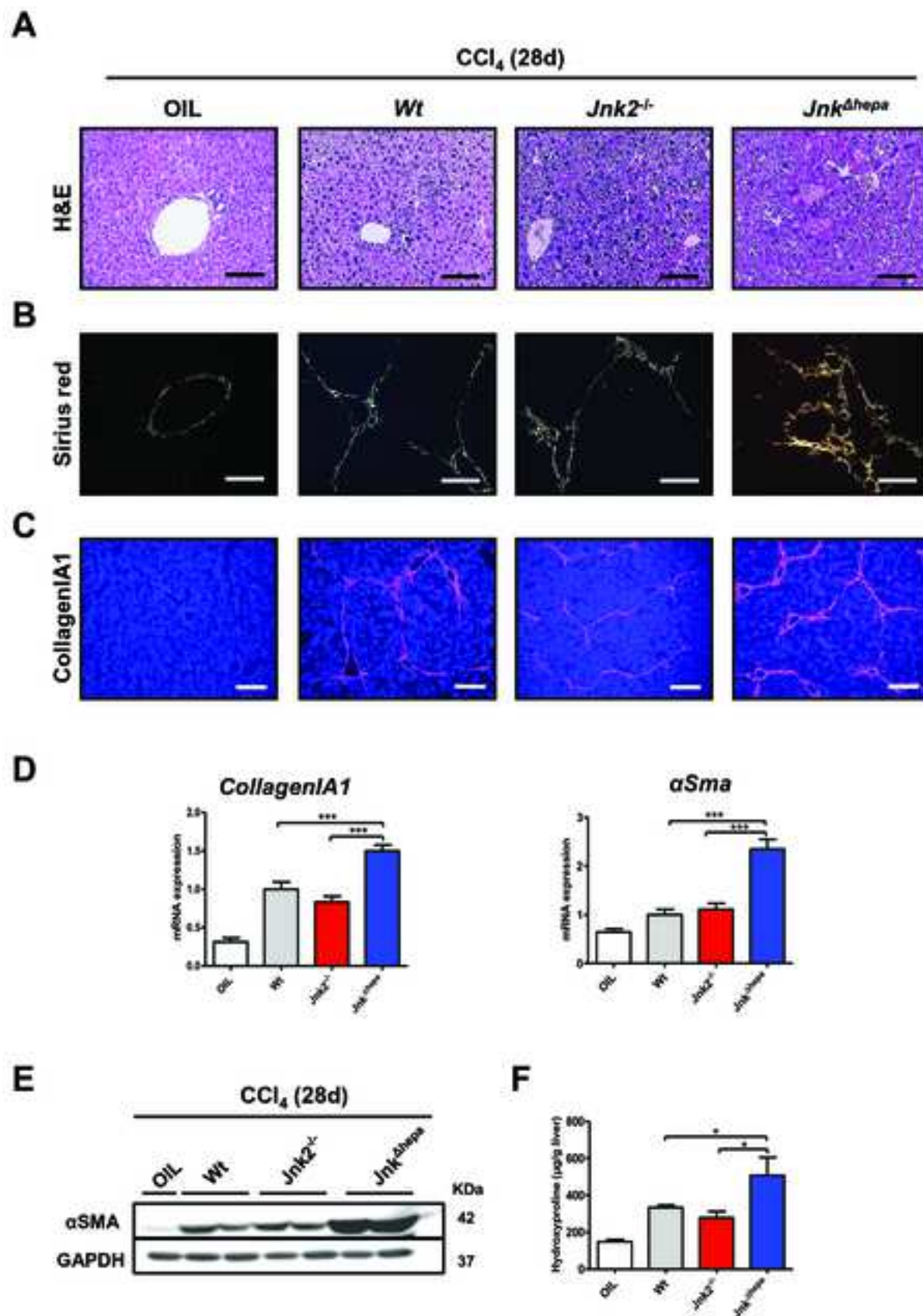


Figure 3

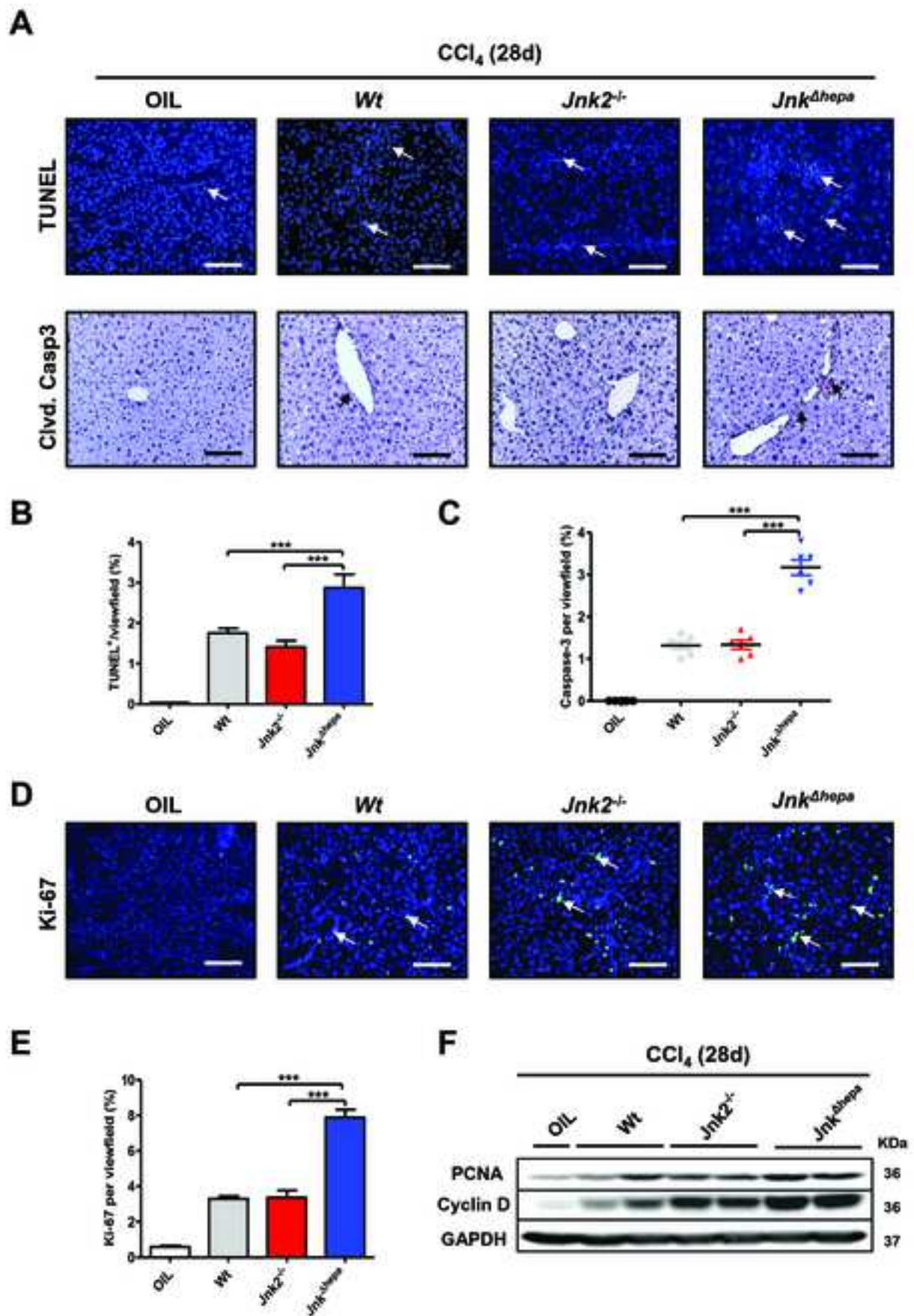


Figure 4

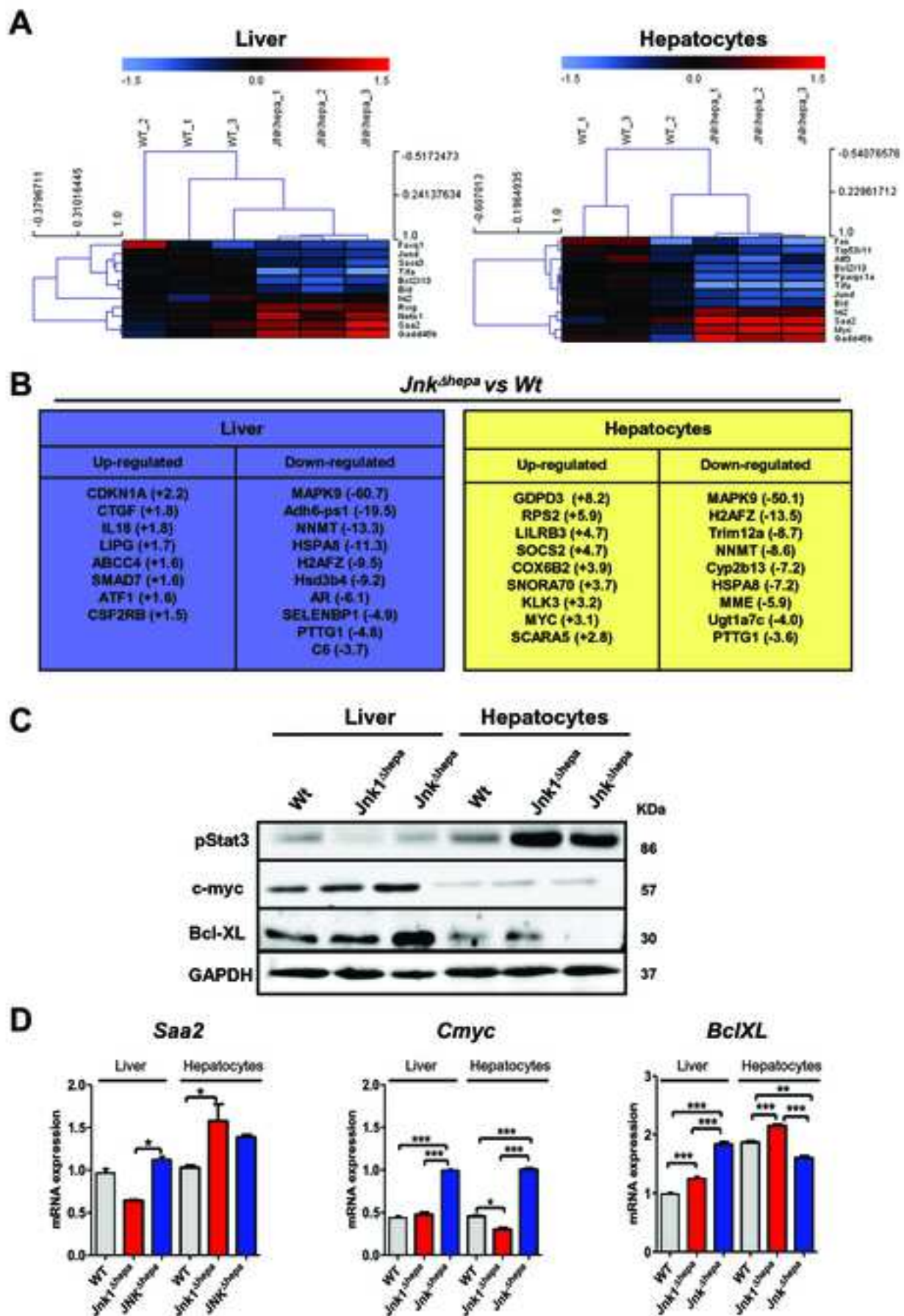
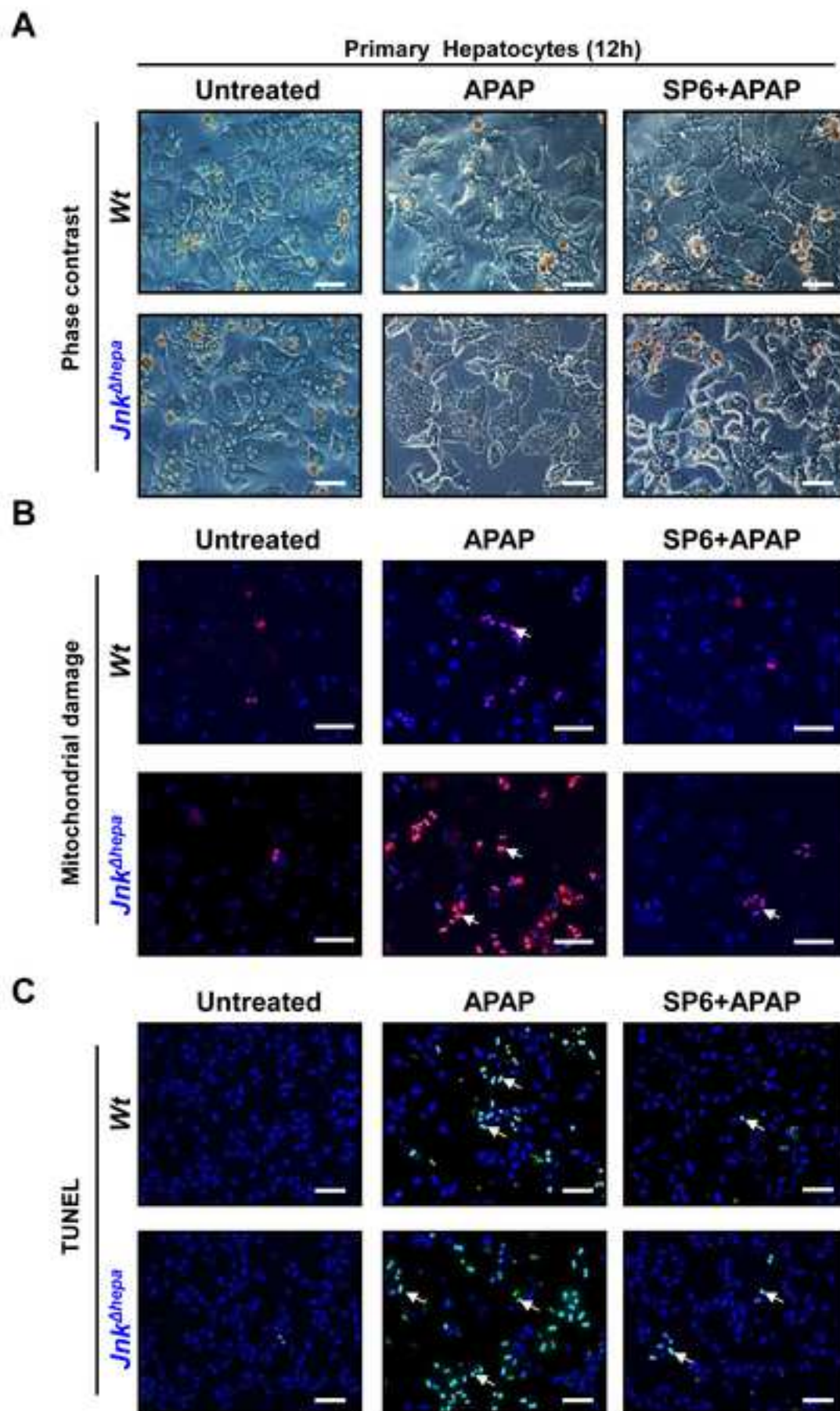


Figure 5



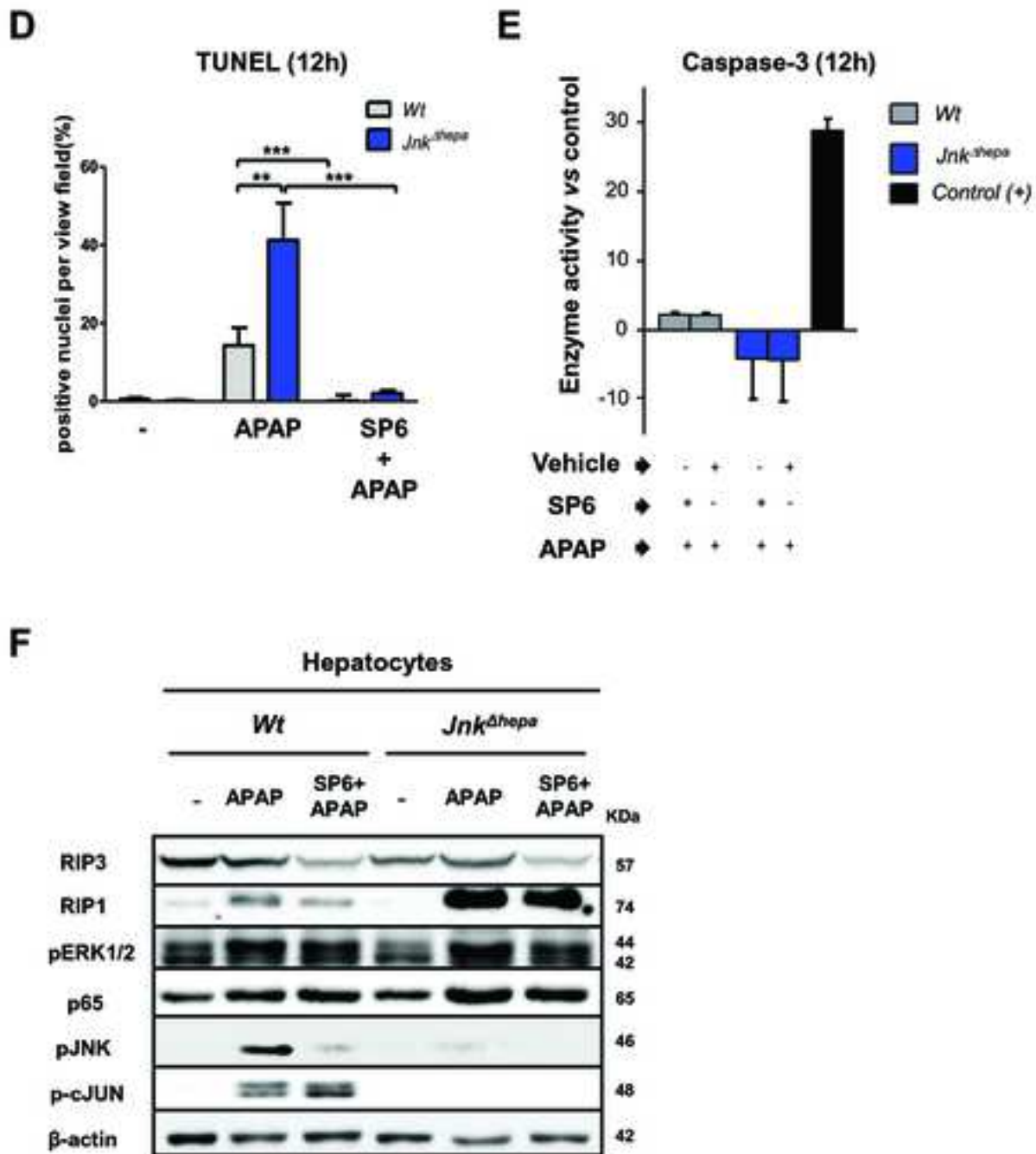


Figure 6 (cont.)

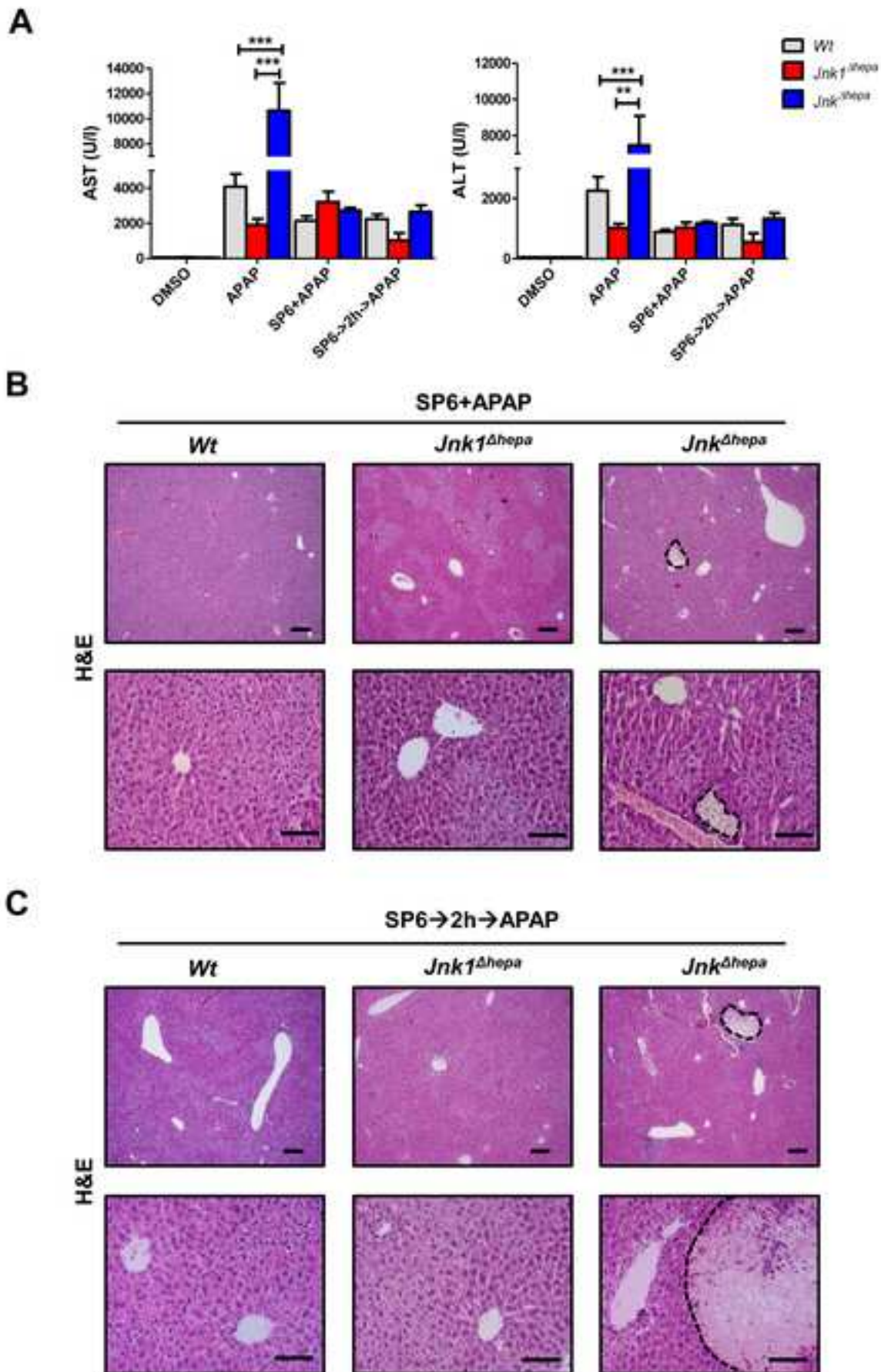


Figure 7

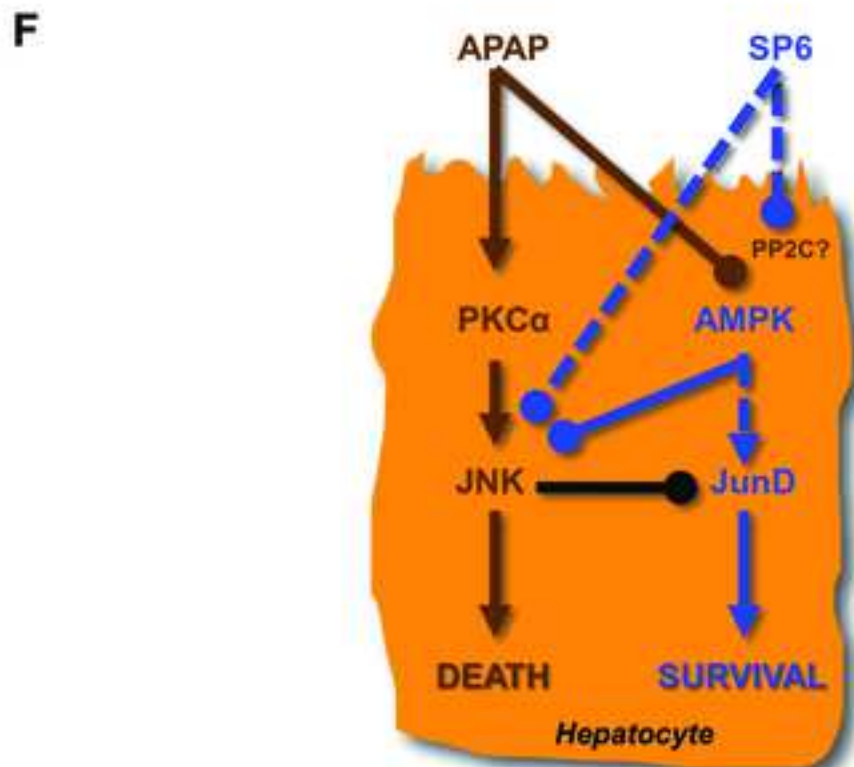
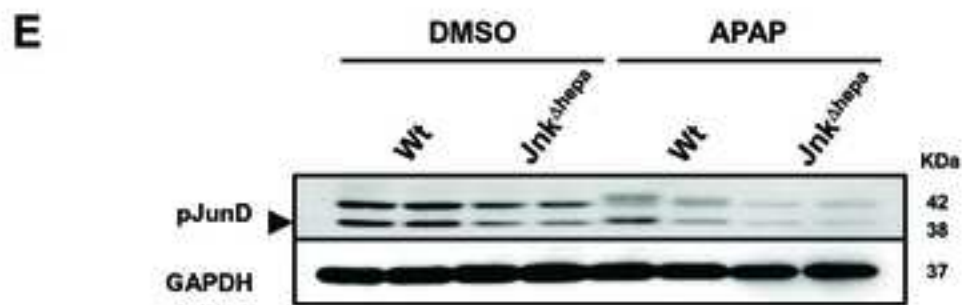
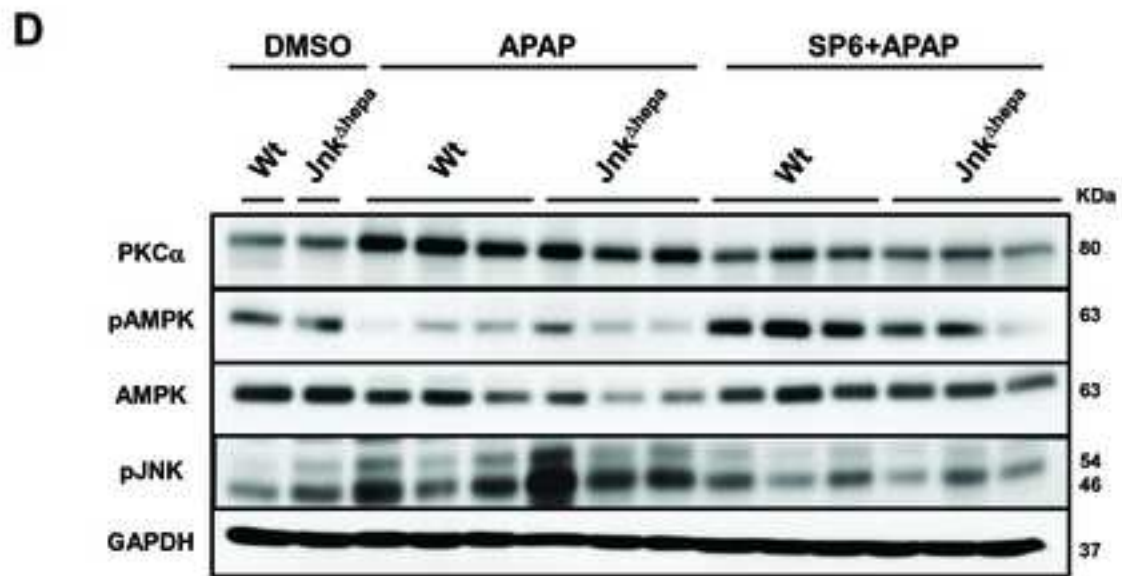


Figure 7 (cont.)

SUPPLEMENTARY INFORMATION

Combined activities of JNK1 and JNK2 in hepatocytes

protect against toxic liver injury

Short Title: Redundancy of JNK1 and JNK1 in hepatocytes

Francisco Javier Cubero; Miguel Eugenio Zoubek; Jin Peng; Wei Hu; Gang Zhao;
Yulia A. Nevzorova; Malika Al Masaoudi; Lars P. Bechmann; Mark V. Boekschoten;
Michael Muller; Christian Preisinger; Nikolaus Gassler; Ali E. Canbay; Tom Luedde;
Roger J. Davis; Christian Liedtke; Christian Trautwein

SUPPLEMENTARY MATERIAL AND METHODS

Isolation and culture of primary hepatocytes

Primary mouse hepatocytes were isolated from 7-8 week-old mice by collagenase perfusion. Living cells were plated on collagen-precoated petri dishes at a density of $1.5 \times 10^4/\text{cm}^2$ in DMEM medium (PAA Laboratories GmbH, Pasching, Austria) supplemented with L-glutamine, high glucose (4.5 g/l), 10% FBS and 100 U/ml penicillin/streptomycin. After 4 h incubation (37°C, 5% CO₂) and every 2 days, medium was renewed. Hepatocytes were cultured up to 4 days.

Quantitative real-time PCR (qPCR)

Total RNA from liver tissues or cultured cells was isolated using Trizol reagent (Invitrogen, Karlsruhe, Germany). Due to low RNA amount in cultured cells, RNeasy Lipid Tissue Mini Kit was used to collect and purify RNA. Reverse-transcription was

performed using an Omniscript RT Kit (Qiagen). Relative quantitative gene expression was measured via real-time PCR using a 7300 Real Time PCR System with SDS software 1.3.1 (Applied Biosystems, Foster City, CA) and a SYBR Green PCR Kit (Invitrogen, Carlsbad, CA). GAPDH expression was used as internal standard. Primer sequences can be provided upon request.

Histological evaluation and immunofluorescence staining

Hepatic tissue were fixed in 4% paraformaldehyde (PFA) immediately after extraction, embedded in paraffin, sectioned and stained for H&E or Sirius red. Samples were reviewed by a blinded pathologist who analyzed the degree of liver injury. The percentage of Sirius red area fraction in all animals was quantified on 10 or 20 low-power (magnification, X10) fields per slide, using the NIH ImageJ® software (<http://rsbweb.nih.gov/>). Immunohistochemistry for CK-19 (DAKO, Hamburg, Germany), α SMA (Sigma, Steinheim, Germany), phospho-JNK (Cell Signaling, Danvers, MA) and F4/80 (Serotec, Dusseldorf, Germany) on paraffin sections, was performed using a Leica automatic stainer (Wetzlar, Germany). For the immunofluorescence staining, frozen cryosections were incubated with Ki-67 (Santa Cruz, Heidelberg, Germany), Collagen IA1 (Bio trend, Cologne, Germany) or *in situ* cell death detection kit (Roche, Mannheim, Germany) and incubated with fluorescence labelled secondary antibodies (AlexaFluor 488 and 564, Invitrogen, Carlsbad, CA, USA). All fluorescence-labelled cryosections were analyzed and documented using an Imager Z1 fluorescence microscope together with Axiovision software (Carl Zeiss, Jena, Germany).

Immunoblot analysis

Liver tissues were homogenized in ice cold NP40-Buffer containing 50 mM Tri- HCl (pH 7.5), 150 mM NaCl, 0.5% NP-40 and 50 mM NaF freshly supplemented with Complete Mini (Roche), PhosSTOP (Roche), 1 mM orthovanadate and 1 mM pefablock. Protein concentrations were determined by BIO-RAD protein assay (BIORAD). Samples were separated by SDS-PAGE and transferred to a cellulose membrane and probed with antibodies for α SMA (Sigma), COLLAGEN 1A1 (Monosan, Beutelsbach, Germany), PCNA (Dianova GmbH, Hamburg, Germany), CYCLIN A (Santa Cruz), CYCLIN D1, BCLXL and PKC α (Santa Cruz), JNK1, JNK2, pJNK (pT183/Y185), P38, CMYC, STAT3, pAMPK, AMPK and MAPK/CDK Substrates (PXP*P or S*PXR/K) (34B2) (Cell Signaling), and GAPDH (Biorad, Munich, Germany). As secondary antibodies, anti-rabbit-HRP (Cell Signaling) and anti-mouse-HRP (Santa Cruz) were used.

Microarray Analysis

Liver and hepatocyte RNA using TRIzol reagent and purified with the RNeasy Mini Kit (Qiagen, Venlo, The Netherlands) according to the manufacturer's instructions was isolated from 8-10 weeks-old male control *Jnk2*^{-/-} and *Jnk*^{Δhepa} mice. Concentrations and purity of RNA samples were determined on a NanoDrop ND-1000 spectrophotometer (Isogen, Maarssen, The Netherlands). RNA integrity was checked on an Agilent 2100 bioanalyzer (Agilent Technologies, Amsterdam, The Netherlands) with 6000 Nano Chips. RNA samples from 3 mice per experimental group were used for microarray analysis. Samples were hybridized on Affymetrix GeneChip Mouse Genome 430 2.0 arrays in the microarray core laboratory of the Nutrigenomics Consortium at Wageningen University, The Netherlands. Hybridization, washing, and scanning of the arrays were performed according to standard Affymetrix protocols.

Array images were processed using packages from the Bioconductor project¹. Probe sets were redefined according to Dai². Probes were assigned to unique gene identifiers, in this case Entrez IDs. Arrays were normalized with the Robust Multi-array Average (RMA) method. Differentially expressed probe sets were identified using intensity-based moderated paired t-statistics. *P* values were corrected for multiple testing using a false discovery rate (FDR) method. Detailed descriptions of the applied methods are available on request.

Peptide lysis, dimethyl-labelling, phosphopeptide enrichment and LC-MS/MS analysis

Primary hepatocytes were scraped off the cell culture dishes after APAP/DMSO treatment, washed three times in ice-cold PBS and lysed in 8M urea (in 50mM ammonium bicarbonate), containing protease and phosphatase inhibitor cocktails (Serva, Heidelberg, Germany) for 30 min on ice and cleared by centrifugation at 20000 g, for 15 min at 4°C. After determination of protein concentration using a BCA assay (Thermo, Waltham, MA) the individual lysates (500 µg each) are reduced with DTT, alkylated with iodoacetamide, and proteolytically digested with the protease Lys-C (1:100, w/w) in 8M urea for 4h at 37°C. Samples were then diluted to 2M urea with 50 mM ammonium bicarbonate and further digested with trypsin (1:75, w/w) overnight at 37°C^{3, 4}. The resulting peptide digests are desalted and dimethyl-labelled “on column”⁵. Control (WT) mice derived peptides are labelled “light”, whereas *Jnk*^{Δhepa} mice derived peptides were labelled “heavy”. The labelled peptide digests are mixed in a 1:1 ratio, dried down and resuspended in 1 M glycolic acid in 80% ACN, 5% TFA). Phosphopeptide enrichment was performed using MagReSyn® Ti-IMAC beads (ReSyn Biosciences, Gauteng, South Africa) according to the manufacturer’s instructions. Samples were then analysed on a nanoLC-MS/MS System (LC: Ultimate 3000 (Dionex, Dreieich, Germany); MS: Orbitrap Elite

(Thermo)). The raw data obtained from the mass spectrometer were processed and quantified with MaxQuant (version 1.4.1.2). The relevant MS and MS/MS spectra were searched against a forward-decoy Swissprot Homo sapiens database (version 09/2014).

Transplantation of bone marrow-derived cells

We transferred bone marrow from *Jnk^{Δhepa}* and control (WT) mice into 6 week-old *Jnk^{Δhepa}* and control isogenic recipients (n=6-7 mice per group) after ablative γ -irradiation, as described previously⁶. Two months after BMT mice were subjected to either 4 weeks treatment with CCl₄ (0.6 mL/kg body weight, diluted in corn oil, injected intraperitoneally every 3 days) or BDL. At this time, mice were sacrificed and samples collected.

Serum parameters

Alanine aminotransferase (ALT), aspartate aminotransferase (AST), bilirubin and alkaline phosphatase (AP) activity (UV test at 37°C) were measured in the Central Laboratory Facility at University Hospital RWTH Aachen according to standard procedures.

SUPPLEMENTARY TABLES AND FIGURES

Supplementary Table I. Origin and clinical features of liver samples from patients with DILI. (f: female; m: male; Bili: total bilirubin; GLDH: glutamate dehydrogenase; TPT: prothrombin time; INR: international normalized ratio; α PTT: activated partial thromboplastin time; NSAID: non-steroidal anti-inflammatory drug).

Supplementary Figure 1. (A) Activation of pJNK in liver samples of patient samples of normal liver human tissue (C3, C4). **(B+C)** PCR blots of tail DNA from *Wt* and *Jnk1 Δ hepa* (upper panel) and control (*Wt*), *Jnk2 $^{-/-}$* , and *Jnk Δ hepa* (lower panel) mice confirmed the respective phenotype of interest.

Supplementary Figure 2. (A+B) A basal study of untreated female (♀) and male (♂) 8-week-old control (*Wt*) or *Jnk Δ hepa* mice was performed. Representative macroscopic view of livers (scale bars: 10mm) and H&E staining of liver sections (scale bars 100 μ m) from each mice group is shown. **(C+D)** Serum AST and ALT was represented in a graph. **(E+F)** Liver weight (LW) and body weight of these mice is shown, and the liver *versus* body weight ratio (%LW/BW) calculated.

Supplementary Figure 3. (A) Control (*Wt*), *Jnk1 Δ hepa* and *Jnk Δ hepa* mice were injected with APAP for 8h and sacrificed. The liver *versus* body weight ratio (%LW/BW) was then calculated. **(B)** Isoprostanes, indicators of lipid peroxides were measured in livers of 8h APAP-treated control (*Wt*) and *Jnk Δ hepa* mice, and represented as pg/ml. **(C)** Densitometry analysis of the protein expression levels of P38 was performed in these mice and represented as arbitrary units of fluorescence (AUF).

Supplementary Figure 4. (A) Control (*Wt*) or *Jnk Δ hepa* mice were injected with GalN and 30 min later with LPS. 8h thereafter mice were sacrificed. **(B)** Survival curve of

control (*Wt*) or *Jnk* ^{Δ hepa} mice treated with GalN+LPS and sacrificed 8h later. **(C)** Serum levels of AST, ALT and GLDH were determined after GalN+LPS-treated control (*Wt*) or *Jnk* ^{Δ hepa} mice. **(D)** Macroscopic (upper panel; Scale bars: 10mm) and microscopic (lower panel; Scale bars: 100 μ m) appearance of control (*Wt*) or *Jnk* ^{Δ hepa} mice after 8h GalN+LPS treatment **(E)** The percentage of liver vs body weight ratio was calculated and represented in a graph.

Supplementary Figure 5. **(A)** Representative macroscopic view of control (*Wt*), *Jnk2*^{-/-} and *Jnk* ^{Δ hepa} livers, 28 days after repeated injections of CCl₄. Corn-oil injections were used as controls. **(B)** Representative Sirius red staining of paraffin sections from the same livers. **(C+D)** Quantification of Sirius red and CollagenIA1 stainings were performed using Image J[®] Software and represented as percentage of area fraction. **(E)** Densitometry analysis of the protein expression levels of α SMA was performed in these mice and represented as arbitrary units of fluorescence (AUF). **(F)** mRNA levels of *Timp1* and *Mmp2* were determined by qRT-PCR in liver tissues of (n=5-10). Data are expressed as mean \pm SEM (*p<0.05; **p<0.01; ***p<0.001).

Supplementary Figure 6. Control (*Wt*), *Jnk2*^{-/-} and *Jnk* ^{Δ hepa} livers were subjected for 4 weeks of repeated CCl₄ injections. **(A)** mRNA levels of *Pcna* were determined by qRT-PCR in liver tissues (n=6-8; **p<0.01). **(B)** Densitometry analysis of the protein expression levels of PCNA and CyclinD was performed in these mice and represented as arbitrary units of fluorescence (AUF).

Supplementary Figure 7. The inflammatory profile is increased in absence of JNK in hepatocytes. **(A)** Representative CD11b staining performed on frozen liver sections of control (*Wt*), *Jnk2*^{-/-} and *Jnk* ^{Δ hepa} livers after 4 weeks of repeated CCl₄ injections.

Scale bars: 100 μ m. Quantification of positive cells was performed in 7-10 view-fields. **(B)** Representative F4/80 staining performed on frozen liver sections of the same livers. Scale bars: 100 μ m. Quantification of F4/80 positive cells per view field is shown. mRNA levels of *IL1 α* **(C)**, *IL1 β* **(D)**, *Mcp1* **(E)** and *Tnf α* **(F)** were determined by qRT-PCR in liver tissue (n=6-8). Data are expressed as mean \pm SEM (*p<0.05; **p<0.01; ***p<0.001).

Supplementary Figure 8. Venny diagram shows comparative gene expression overlap in untreated 8 week-old control (*Wt*) and *Jnk Δ *hepa** livers and primary hepatocytes. **(A)** Up-regulated genes. **(B)** Down-regulated genes. **(C+D)** Validation of gene array analysis by mRNA expression was performed in liver tissue and primary hepatocytes of 8 week-old untreated control (*Wt*), *Jnk1 Δ *hepa** and *Jnk Δ *hepa** mice. The mRNA expression levels *Bad* and *Jnk2* are shown (*p<0.05; **p<0.01; ***p<0.001).

Supplementary Figure 9. (A) Primary hepatocytes were isolated from control (*Wt*), *Jnk2 $^{-/-}$* and *Jnk Δ *hepa** mice. A total number of 500.000 cells were seeded in 6-well plates and cultivated for up to 48h. Visible light microphotographs were taken in untreated hepatocytes. Scale bars: 100 μ m. **(B)** Representative TUNEL stainings of primary hepatocytes. Dead cells are stained green; total cells were counter-stained with DAPI (blue). Scale bars: 100 μ m. **(C)** Staining for BrdU was performed in coverslips and counterstained to DAPI (blue). Scale bars: 100 μ m. **(D)** BrdU-positive cells were counted in untreated control (*Wt*) and *Jnk Δ *hepa** hepatocytes, and displayed in a graph.

Supplementary Figure 10. Primary hepatocytes were isolated from control (*Wt*) and *Jnk Δ *hepa** mice. A total number of 500.000 cells were seeded in 6-well plates and cultivated for up to 12h. **(A)** Reactive oxygen species (ROS) were measured in

presence or absence of APAP and/or SP600125, an inhibitor of the JNK pathway. **(B)** Annexin V (green)/Ethidium Homodimer III (red)/DAPI (blue) was performed and microphotographs were taken. **(C)** Quantification of the double Annexin V/Ethidium Homodimer III/ DAPI-positive cells was graphed. Values are mean \pm SEM from at least 6 mice per group (* p <0.05; ** p <0.01).

Supplementary Figure 11. (A) Hepatocytic protein extracts from 8h-APAP-treated control (*Wt*) and *Jnk* ^{Δ hepa} primary hepatocytes were labelled with beads, digested with trypsin, and the phosphopeptides were enriched, and analyzed using mass spectrometry. **(B)** The expression of phosphoMAPK/CDK substrates was assessed in untreated and 8h-APAP-treated control (WT) and *Jnk* ^{Δ hepa} primary hepatocytes. Potential target proteins of JNK with matching molecular weights are displayed on the right. Values are mean \pm SEM from at least 6 mice per group (** p <0.01 and *** p <0.001).

SUPPLEMENTARY REFERENCES

1. Gentleman RC, Carey VJ, Bates DM, Bolstad B, Dettling M, Dudoit S, Ellis B, Gautier L, Ge Y, Gentry J, Hornik K, Hothorn T, Huber W, Iacus S, Irizarry R, Leisch F, Li C, Maechler M, Rossini AJ, Sawitzki G, Smith C, Smyth G, Tierney L, Yang JY, Zhang J. Bioconductor: open software development for computational biology and bioinformatics. *Genome Biol* 2004;5:R80.
2. Dai M, Wang P, Boyd AD, Kostov G, Athey B, Jones EG, Bunney WE, Myers RM, Speed TP, Akil H, Watson SJ, Meng F. Evolving gene/transcript definitions significantly alter the interpretation of GeneChip data. *Nucleic Acids Res* 2005;33:e175.
3. Preisinger C, Schwarz JP, Bleijerveld OB, Corradini E, Muller PJ, Anderson KI, Kolch W, Scholten A, Heck AJ. Imatinib-dependent tyrosine phosphorylation profiling of Bcr-Abl-positive chronic myeloid leukemia cells. *Leukemia* 2013;27:743-6.
4. Scholten A, Preisinger C, Corradini E, Bourgonje VJ, Hennrich ML, van Veen TA, Swaminathan PD, Joiner ML, Vos MA, Anderson ME, Heck AJ. Phosphoproteomics study based on in vivo inhibition reveals sites of calmodulin-dependent protein kinase II regulation in the heart. *J Am Heart Assoc* 2013;2:e000318.
5. Boersema PJ, Raijmakers R, Lemeer S, Mohammed S, Heck AJ. Multiplex peptide stable isotope dimethyl labeling for quantitative proteomics. *Nat Protoc* 2009;4:484-94.

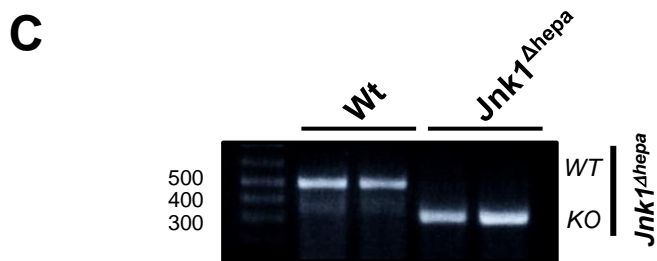
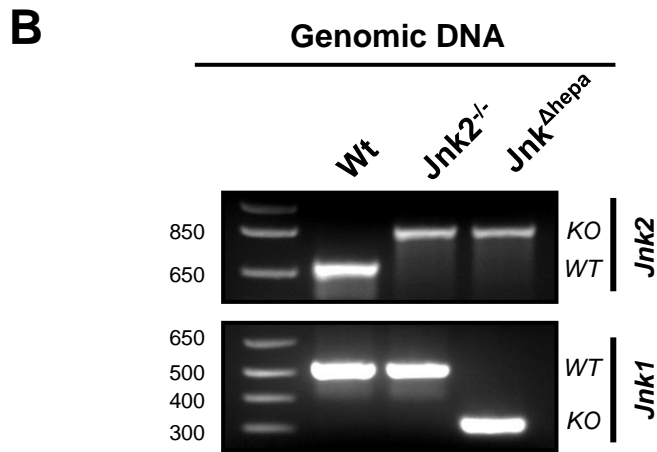
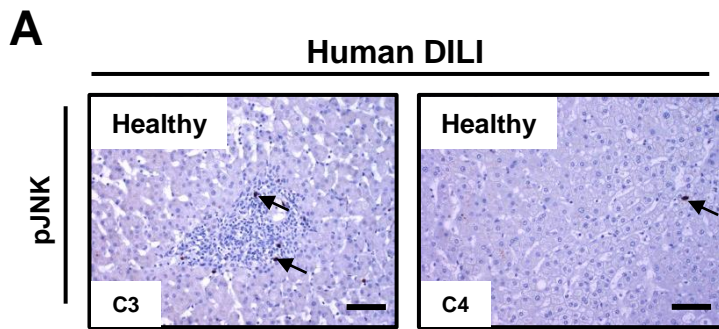
6. **Berres ML, Koenen RR**, Rueland A, Zaldivar MM, Heinrichs D, Sahin H, Schmitz P, Streetz KL, Berg T, Gassler N, Weiskirchen R, Proudfoot A, Weber C, Trautwein C, Wasmuth HE. Antagonism of the chemokine Ccl5 ameliorates experimental liver fibrosis in mice. *J Clin Invest*;120:4129-40.

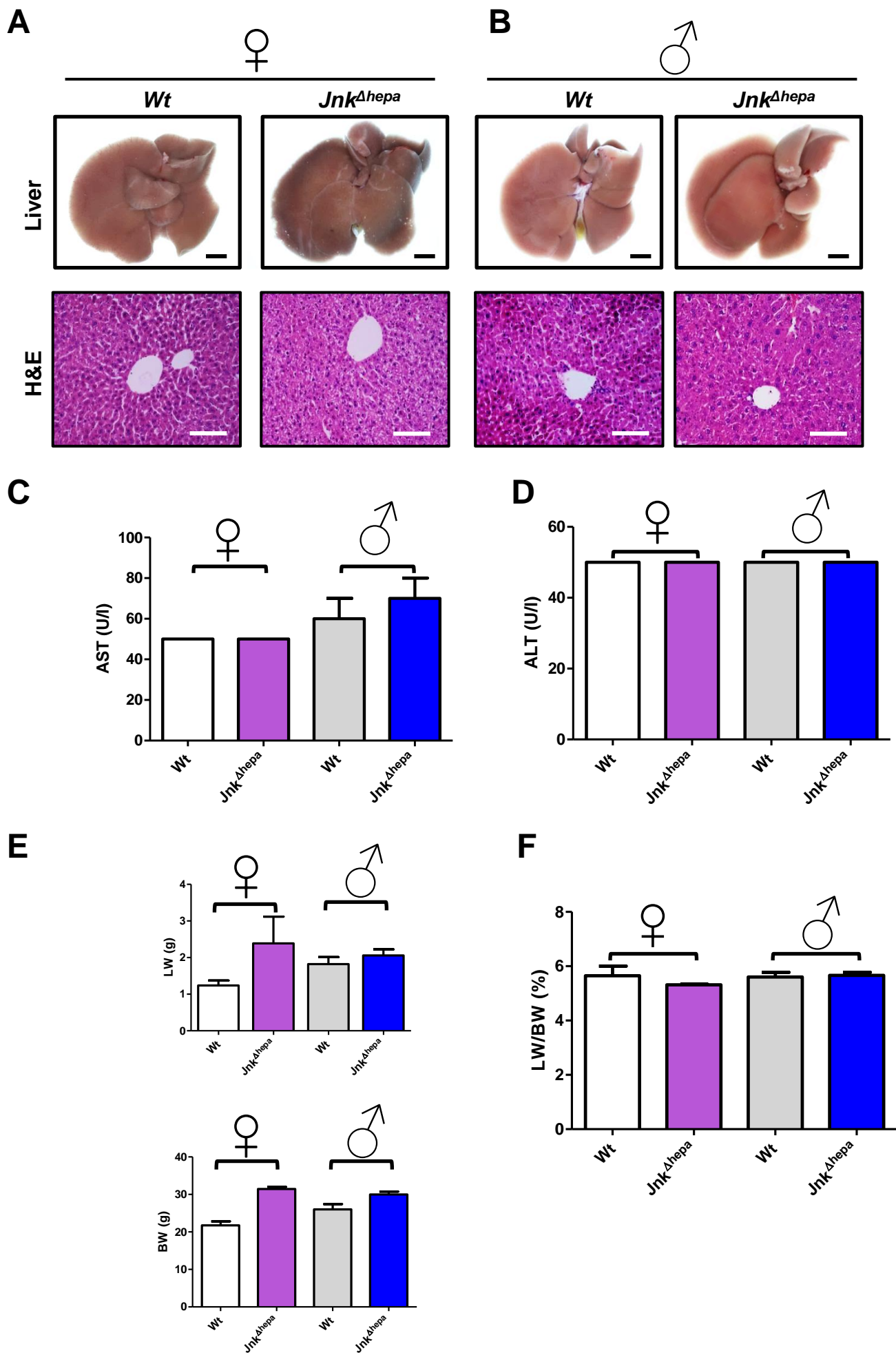
Author names in bold designate shared co-first authors

Suppl. Table I

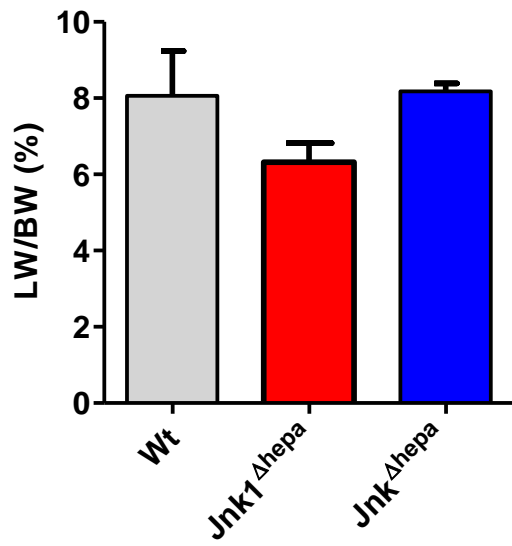
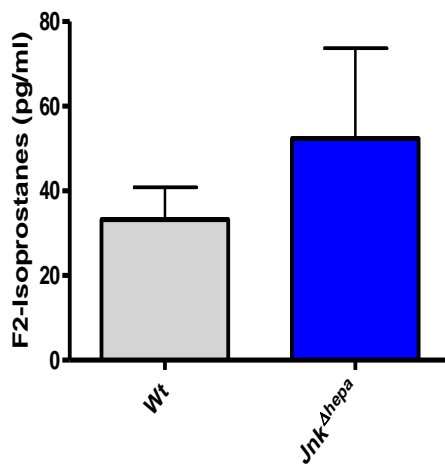
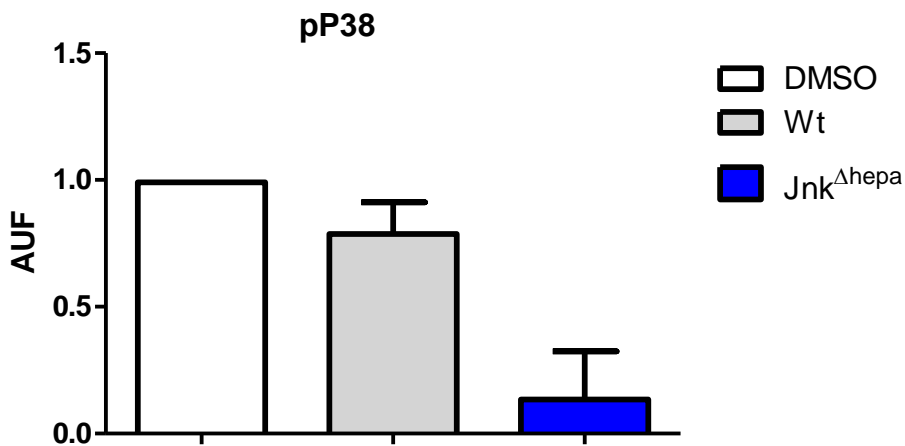
#	Sex	Age	Etiology	AST	ALT	Bili	GLDH	AP	GGT	TPT	INR	αPTT	Creatine	Phosphate
				<i>U/l</i>	<i>U/l</i>	<i>mg/dl</i>	<i>U/l</i>	<i>U/l</i>	<i>U/l</i>	<i>%</i>		<i>sec</i>	<i>mg/dl</i>	<i>mg/dl</i>
1	f	50	Paracetamol	16253	4320	3.90	622.60	86	447	17	3.39	56.50	1.01	-
2	f	23	Phenprocoumon	215	154	3.20	-	63	216	42	1.73	48.00	0.94	3.80
3	m	48	Autoimmune	1004	1068	28.50	18.50	141	148	48	1.44	31.70	0.56	2.50
4	f	63	NSAID	189	209	4.30	10.60	85	38	24	2.73	56.40	0.87	3.00

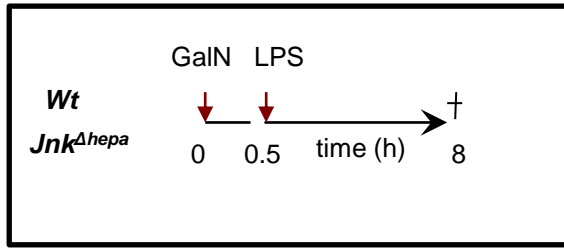
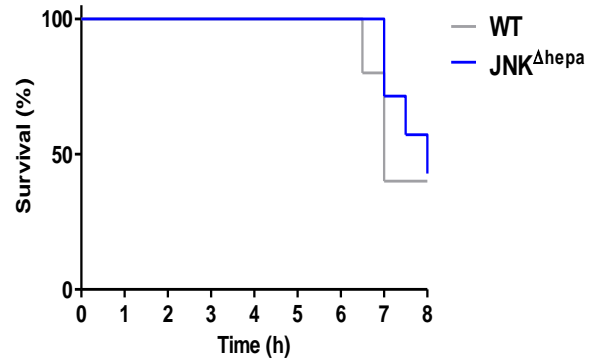
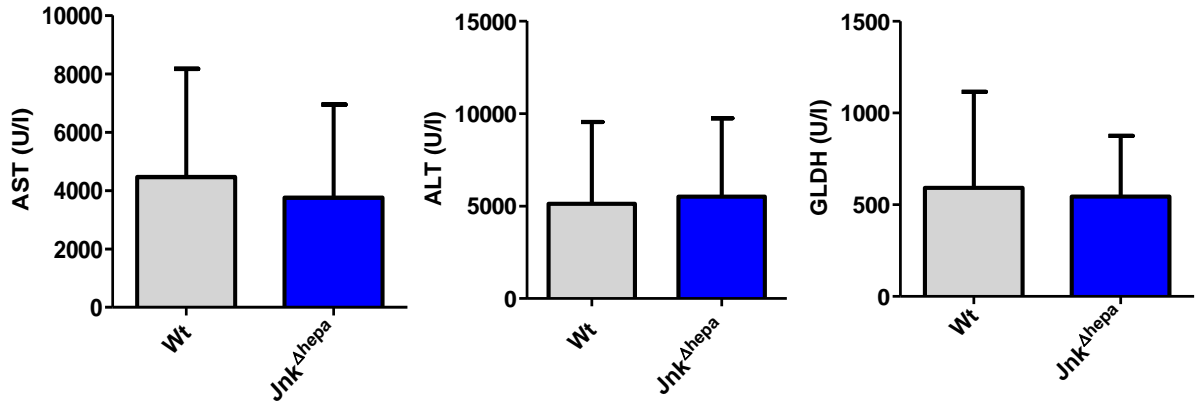
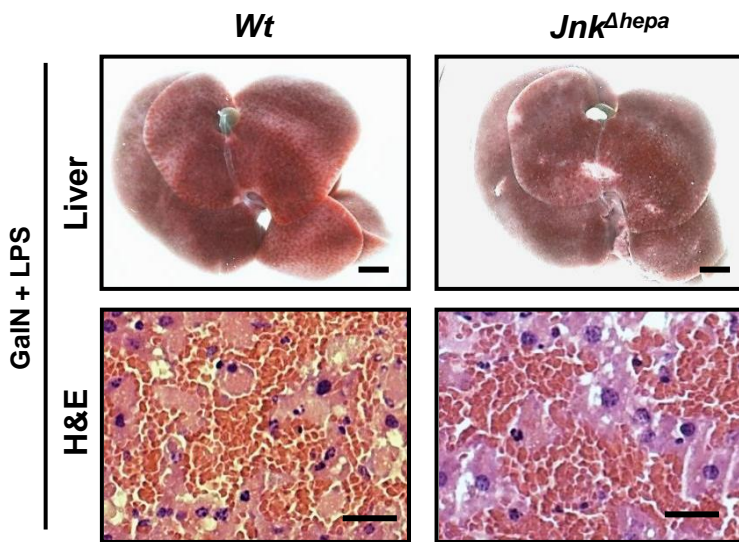
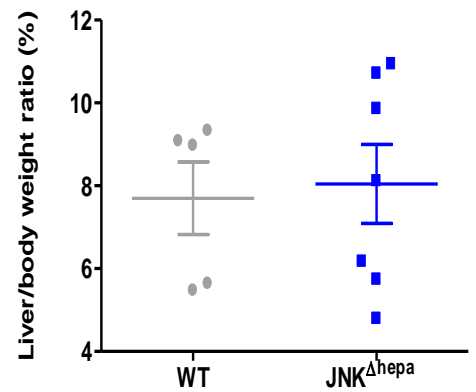
Origin and clinical features of liver samples from patients with DILI. (f: female; m: male; Bili: total bilirubin; GLDH: glutamate dehydrogenase; TPT: prothrombin time; INR: international normalized ratio; αPTT: activated partial thromboplastin time; NSAID: non-steroidal anti-inflammatory drug).





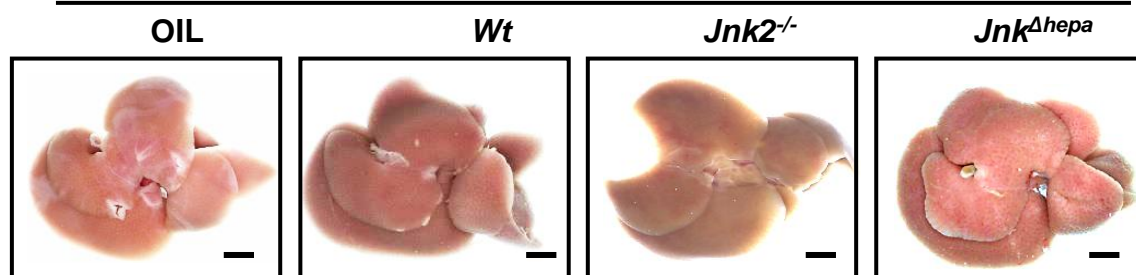
Suppl. Fig. 2

A**B****C**

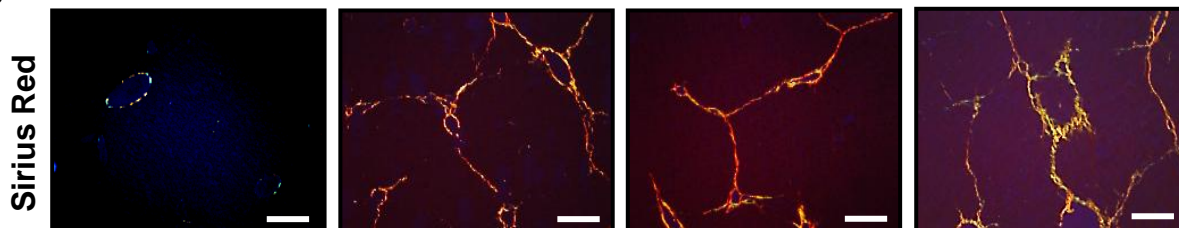
A**B****C****D****E**

CCl₄ (28d)

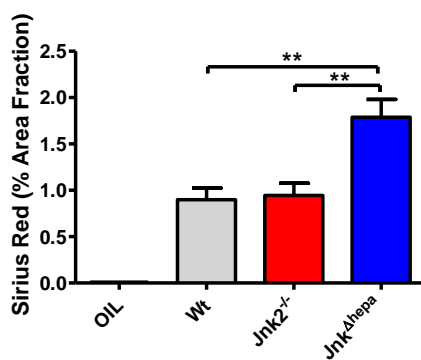
A



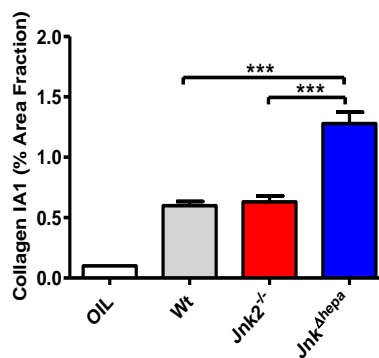
B



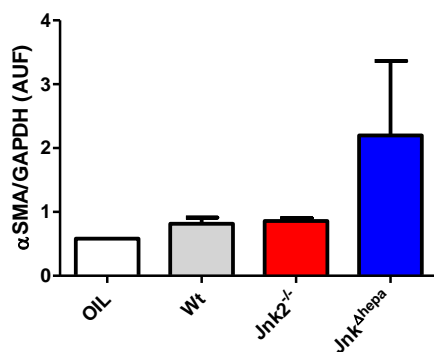
C



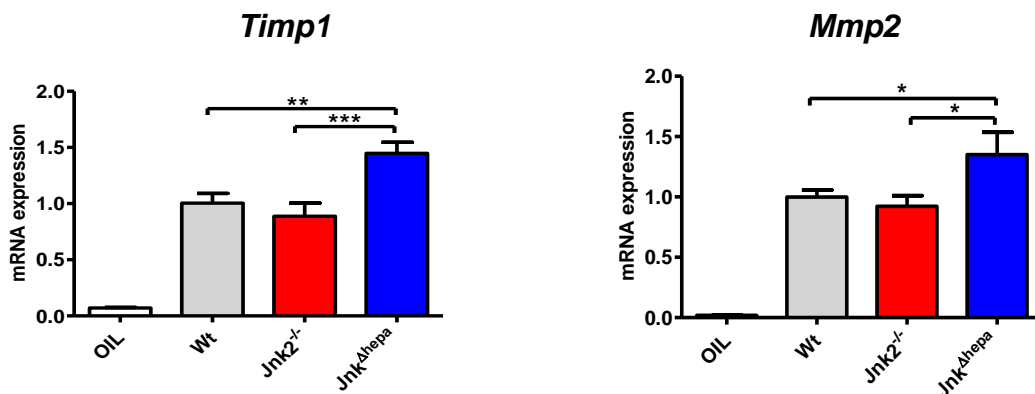
D



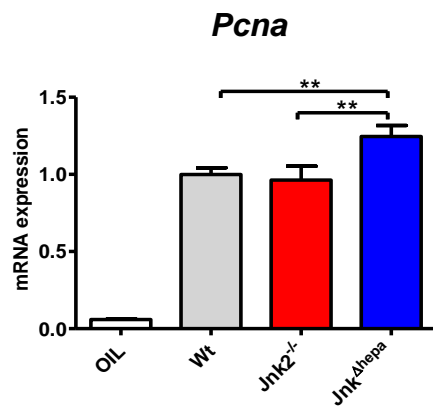
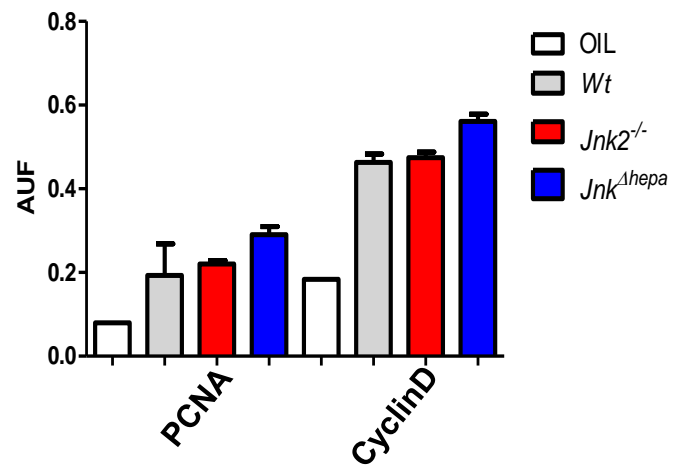
E

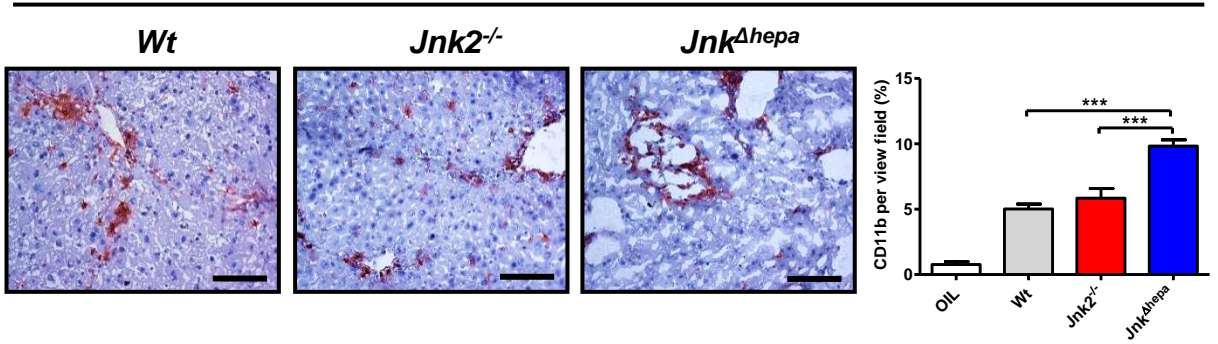
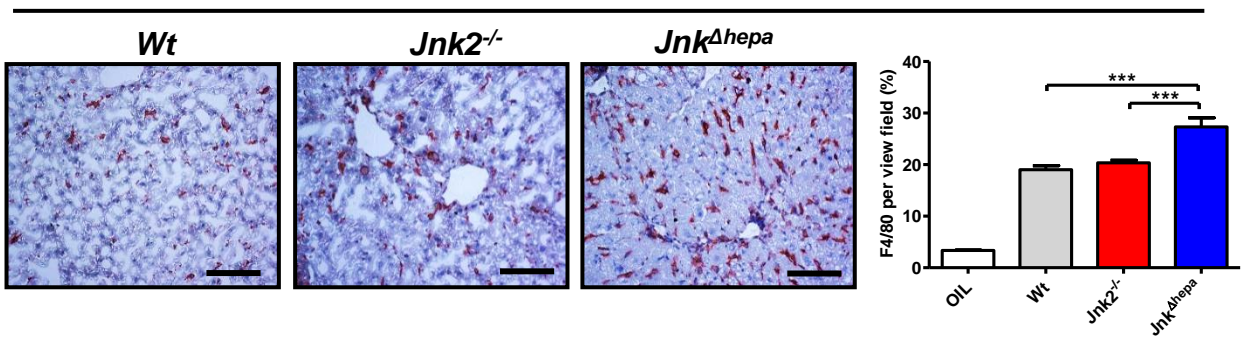
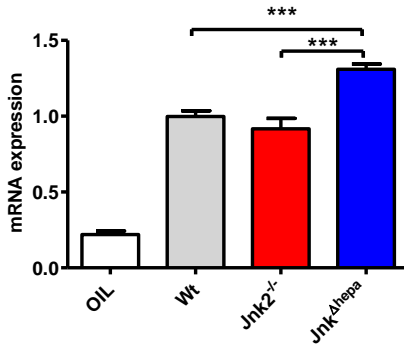
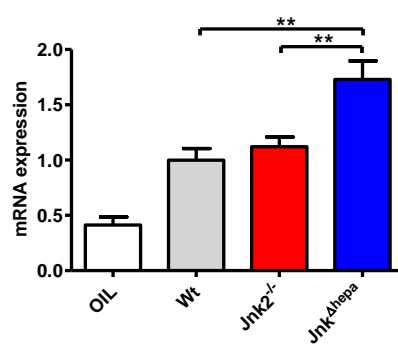
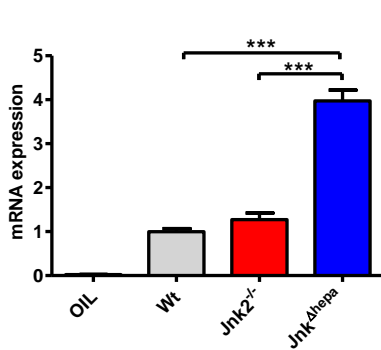
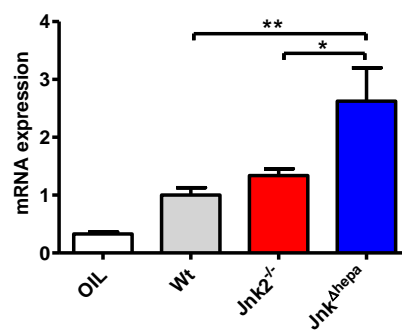


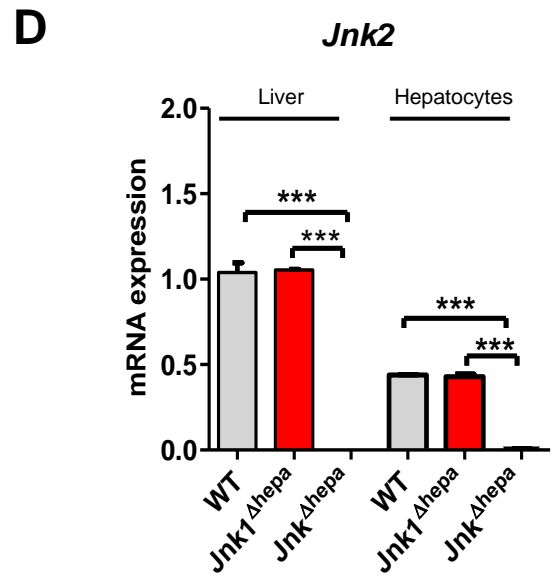
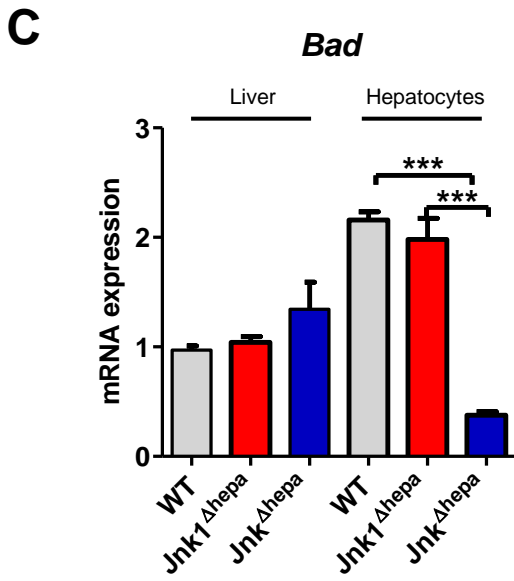
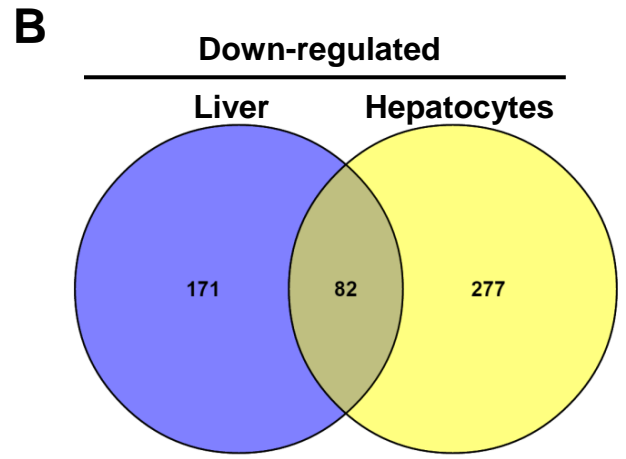
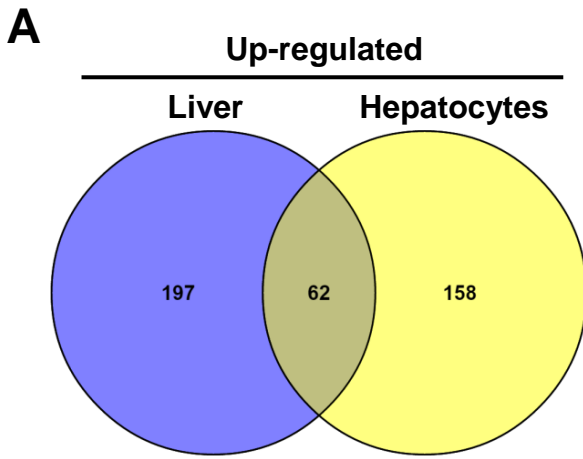
F



Suppl. Fig. 5

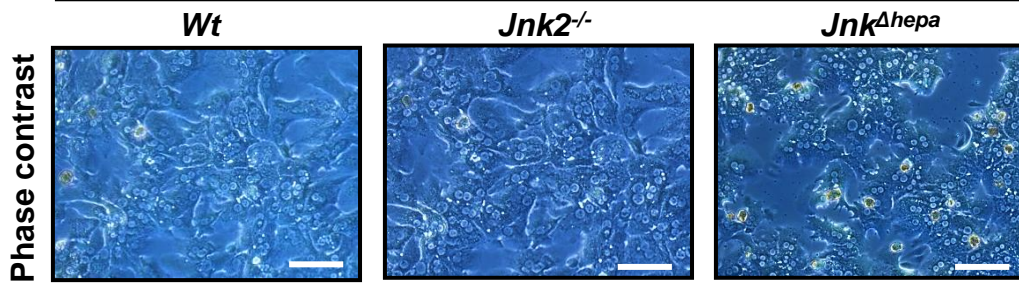
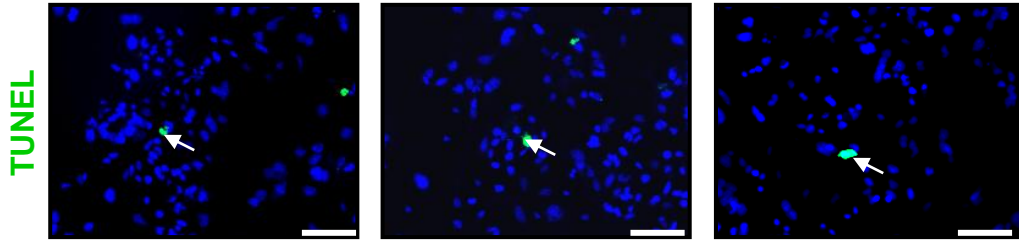
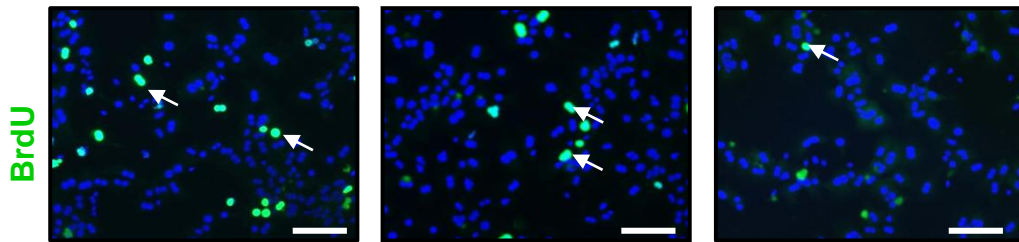
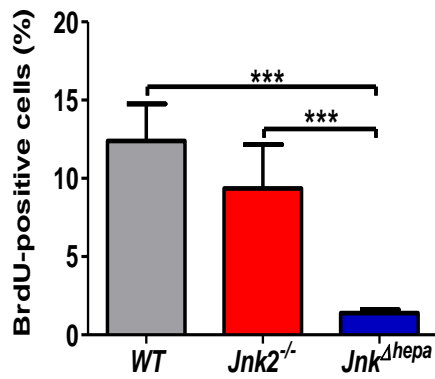
A**B**

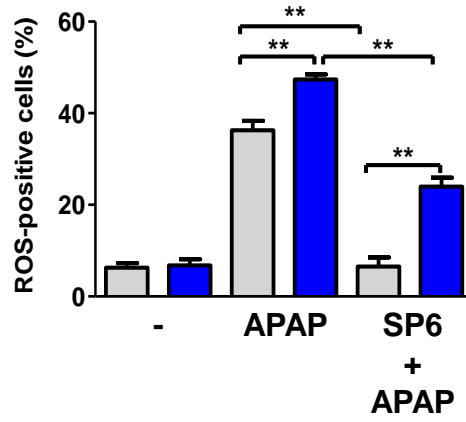
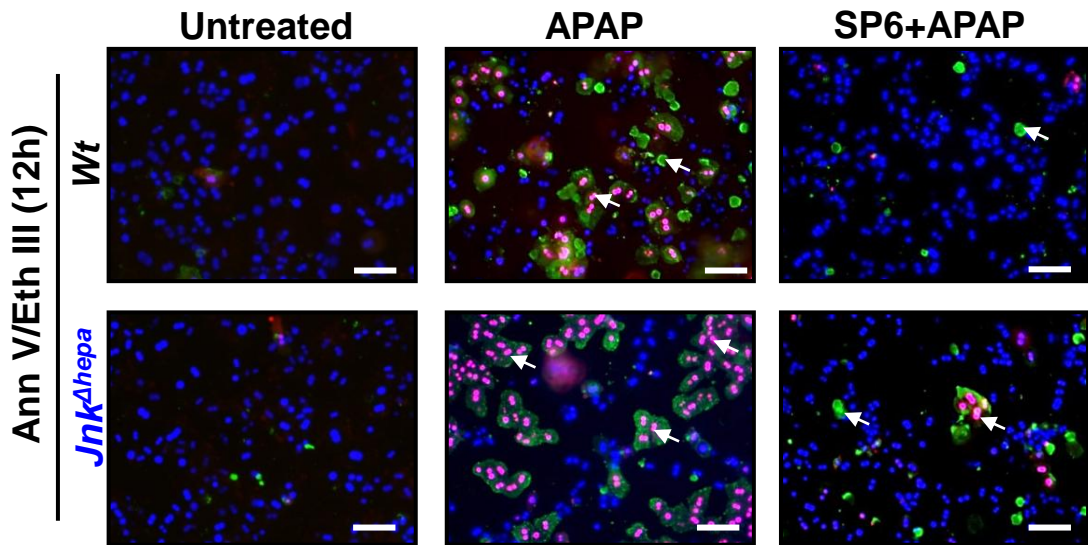
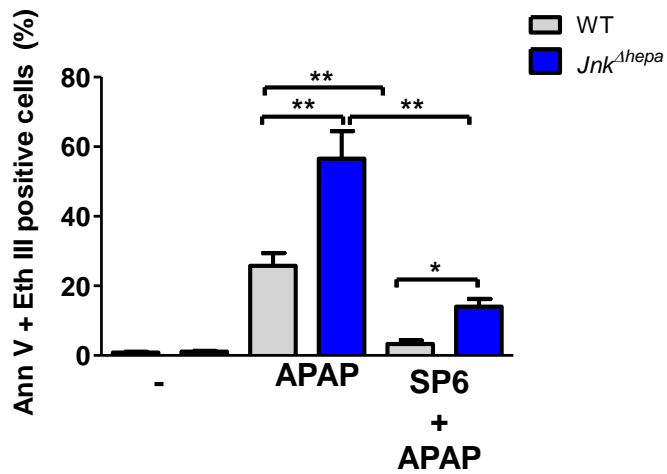
A**CD11b****B****F4/80****C*****IL1α*****D*****IL1β*****E*****Mcp1*****F*****Tnf***

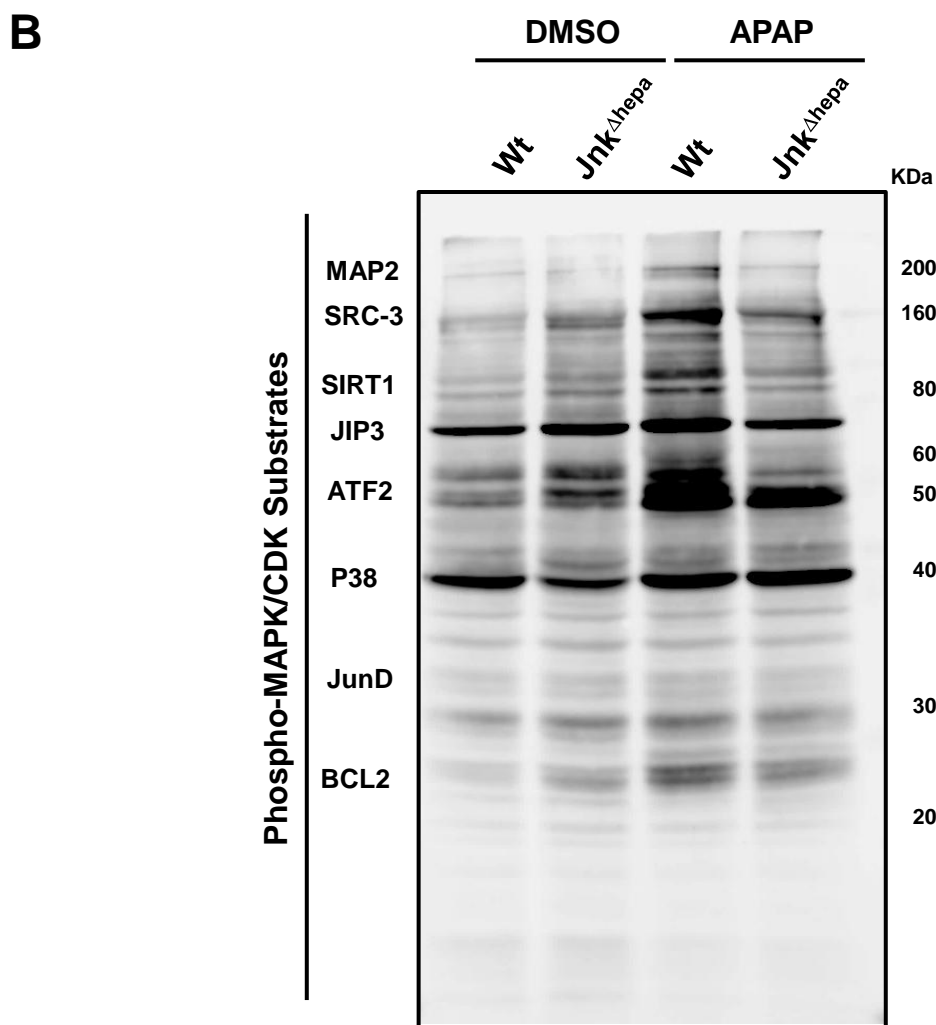
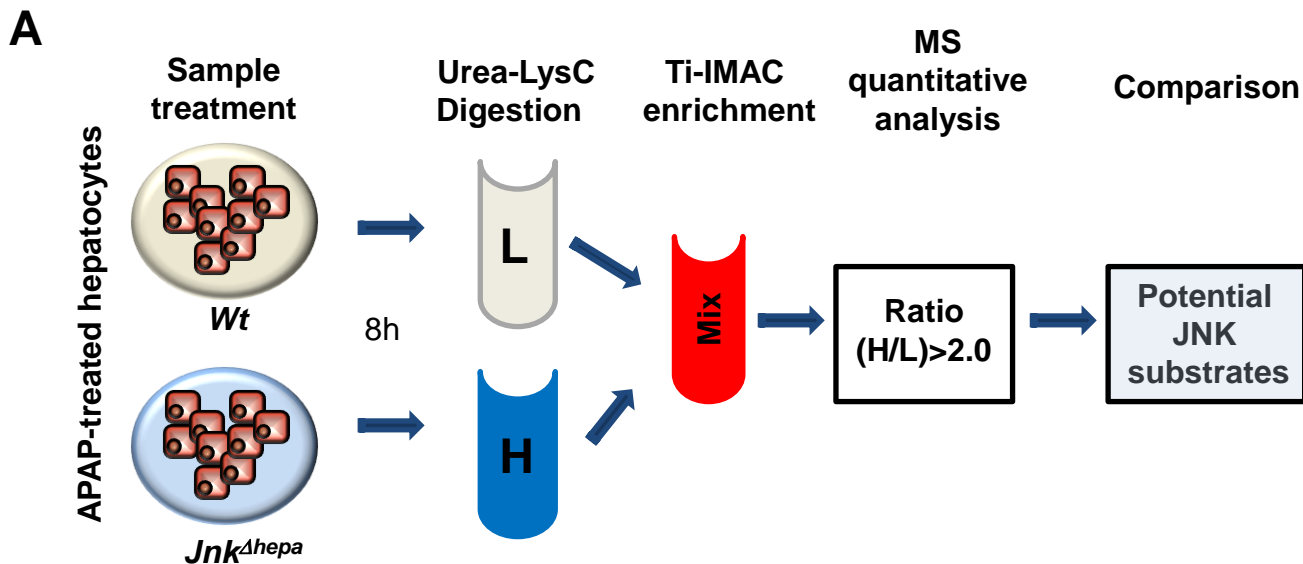


A

Primary Hepatocytes (48h)

**B****C****D**

A**B****C**





Click here to access/download

Revised Manuscript in Word or RTF (no changes marked)

Revised version of the manuscript unmarked.docx